An Inverse Model-Based Approach to Estimate Infiltration in Commercial Buildings Using Occupant-Generated CO_2 And Humidity

by

Zijun Xiong

A thesis submitted to the Faculty of Graduate and Postdoctoral Affairs in partial fulfillment of the requirements for the degree of

Master of Applied Science

in

Civil Engineering

Department of Civil and Environmental Engineering

Carleton University

Ottawa, Ontario

September 2021

Abstract

Air infiltration has a significant impact on building energy performance and the indoor environment. Monitoring air infiltration continuously is of great importance to compare the airtightness of a building over time, and to detect building envelope degradation over time. An accurate estimate of air infiltration rate also informs envelope retrofit decisions to improve airtightness. However, air mobility and other environmental factors, such as wind or indoor-outdoor temperature differences, often make the accurate measurement of air infiltration challenging. Further, conventional air infiltration testing approaches such as fan pressurization and tracer gas tests possess certain drawbacks limiting their applicability in commercial buildings. To address the limitations of air infiltration tests, this research proposes a low-cost inverse model-based approach for estimating air infiltration rates by extracting the occupant-generated carbon dioxide (CO_2) and humidity data from a building automation system (BAS). The laboratory tracer gas concentration decay tests were carried out to explore the effectiveness of replacing sulphur hexafluoride (SF_6) with CO_2 and the appropriateness of using low-cost BAS-grade sensors. Then the applicability of the proposed inverse model-based approach was verified by tracer gas concentration decay tests using both CO_2 and water vapour. In this case, the historical CO_2 and humidity data were used to validate the model to examine whether this approach can estimate infiltration rates from historical data. At last, return air CO_2 concentration data from three air handling units were utilized to demonstrate this novel approach. Different regression models were developed to investigate the suitability of this ubiquitous sensor type to estimate building-level infiltration rates. The results indicated that the proposed method could conveniently lend itself to estimate air infiltration rates at a reasonable accuracy using existing sensor data.

Preface

This integrated thesis includes a journal paper and a conference paper. The journal paper is under review, while the conference paper has been published. Should readers wish to refer to materials from this thesis, the current thesis is required to be cited. The articles included in this thesis are as follow:

- **Article 1** : Z. Xiong; J. Berquist; H. B. Gunay; C.A.Cruickshank. An inquiry into the use of indoor CO_2 and humidity ratio trend data with inverse modelling to estimate air infiltration. *Building and Environment* [Under review].
- **Article 2** : Z. Xiong; H. B. Gunay; C.A.Cruickshank; A. Wills. Estimation of infiltration in commercial buildings based on existing CO_2 sensors: An inverse Approach. *ASHRAE Transactions. 2021, Vol. 127 Issue 1, p30-37. 8p.*

The articles have been altered slightly to help the flow of this dissertation. Reference is made to figures from other chapters to avoid redundancy. Use of copyrighted material from the published articles is acknowledged as per the corresponding publisher's permission guidelines with respect to the authors' rights.

In the aforementioned articles, Zijun Xiong was the principal contributor to the data analysis and preparation of written material and figures presented in the articles, under the supervision of Dr. H. Burak Gunay and Dr. Cynthia A Cruickshank. Justin Berquist and Dr. Adam Wills contributed to critical feedback and review.

Acknowledgments

I would like to express my deepest appreciation to my supervisors Professor Burak Gunay and Professor Cynthia Cruickshank, for their patience, encouragement, and trustworthy guidance. Without their invaluable expertise and insights, I would not have been able to accomplish my research. I also had the great pleasure of working with Justin Berquist and Dr. Adam Wills. Their support and insightful feedback brought my research to a higher level.

I also wish to thank other members at Carleton Building Performance Research Center, especially Narges Torabi, Ipek Yilmaz and Darwish Darwazeh, for their unreserved help during these two years.

This research was funding by the federal government Department of Natural Resources Canada through the Program of Energy Research & Development (PERD) and by the National Research Council Canada.

Finally, I would like to express gratitude to my parents for their unconditional love and support since I was born. Without their unwavering support and encouragement, I would not be able to overcome all the difficulties encountered in studying abroad. Special thanks to my partner, Weihao Liu, whose enthusiasm for life and positive attitude for work motivates me all the time.

Table of content

List of Figure

List of Table

List of Abbreviation

^{41}Ar	Argon isotope
^{85}Kr	Krypton-85
ACH	Air Changes per Hour
AHU	Air Handling Unit
ASHRAE	The American Society of Heating, Refrigerating and Air-Conditioning Engineers
BAS	Building Automation System
CO_2	Carbon Dioxide
HVAC	Heating, Ventilating, and Air Conditioning
IAQ	Indoor Air Quality
IARL	Indoor Air Research Loboratory
PFT	Perfluorocarbon Tracers
RH	Relative Humidity
SF_6	Sulphur Hexafluoride

Chapter 1 - Introduction

1.0 Introduction

Building infiltration plays a crucial role in the lifecycle of buildings due to the concern about the environment. The significant impacts of infiltration on buildings manifest in energy consumption, indoor air quality (IAQ), and building envelope. It is estimated that 41% of the energy in the U.S. is consumed by the building sector, and air infiltration is the third most influential factor [1]. The outdoor air entering a building unexpectedly through building leakages results in thermal discomfort, which may burden the heating, ventilation, and air conditioning (HVAC) system and increase the energy demand for heating or cooling to maintain a comfortable indoor thermal environment [2]. The U.S. Department of Energy reported that in 2010, residential buildings in the U.S. consume 10,023 Petajoules (PJ) of energy to maintain indoor thermal comfort, while the U.S. commercial buildings spend 5,803 PJs of energy on space heating and cooling [1]. Infiltration is also a way to transport outdoor airborne contaminants, such as PM2.5, radon and fungal spores, which can degrade IAQ and impact occupant health [3, 4]. In terms of the building envelope, air infiltration is also a significant cause of concealed moisture condensation. The water vapour in the air is convective through the airflow and condenses at the building envelope components due to the temperature difference between indoor and outdoor, which leads to the change of the properties of building materials and then deteriorates building structure [5, 6].

Accurate measurement of air infiltration rate holds prime importance to identify the resultant effects of high infiltration level rates and to take necessary measures accordingly. With the development of technology, several infiltration measurement techniques were introduced and

applied in the field in the past decades. However, due to the high requirements of measurement apparatus and technicians, most of the techniques are suitable for small residential buildings rather than large commercial and institutional buildings. According to the National Energy Code of Canada for Buildings (NECB) [7], precise airtightness measurement is required for the whole building to detect air leakage. On the other hand, accurate measurements of infiltration are also required in terms of building modelling and energy simulation in design and analysis. Since accurate infiltration rates are difficult to obtain, analysts often treat the inputs of infiltration as default values during the simulation work, which does not capture the full impact of infiltration on commercial buildings. In this regard, there is a necessity for an approach to estimate the air infiltration rates in commercial buildings that has ease of implementation.

1.1 Background

This section firstly reviews the crucial terminologies and metrics, which will appear in this thesis. Then some essential measuring techniques used to measure the infiltration rates are introduced and their advantages and disadvantages.

1.1.1 Terminology and metrics

Infiltration represents the uncontrolled movement of airflows from outdoor to indoor through building leakage locations. It is important to note that the terminology infiltration is used to describe the phenomenon of infiltration and exfiltration, which refers to the uncontrolled airflows that move air from indoor to outdoor. The driving force of infiltration is the pressure differences between indoor and outdoor, which are induced by stack effect, wind-driven pressure and mechanical ventilation system operation.

The stack effect in buildings causes airflow into or out of a building due to the pressure difference caused by the temperature difference between indoor and outdoor. Figure 1.1 illustrates the mechanism of the stack effect in the heating season. During the heating season, the warmer and lighter indoor air rises up and creates positive pressure. The air in the upper portions of the building escapes through the openings at the top of a building (e.g., windows, stack, unintentional openings, etc.) due to positive pressure. Because of the upward air movement, the negative pressure is created at the bottom that draws in the cold outdoor air through unintentional openings at the lower levels of a building. The reverse phenomena occur in the cooling season that the cold indoor air settles down and escapes at the bottom while the hot outdoor air enters the building to replace the upper indoor air. The uncontrolled airflow movements caused by the stack effect result in infiltration.

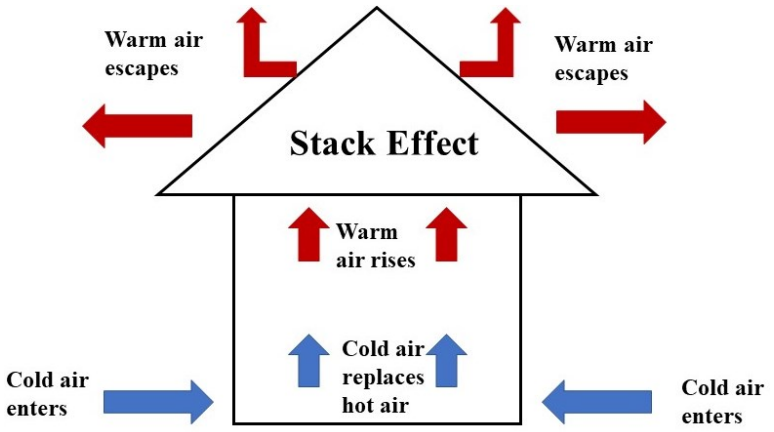

Figure 1.1: Stack effect induced by temperature difference in heating season.

Wind-driven pressure is also a driving force of infiltration. As shown in Figure 1.2, the positive pressure is created when the airflow strikes the windward wall, whereas the negative pressure is created on the leeward wall, the roof and other sides of the house. Due to this pressure difference, the airflow enters the house through openings or building envelope leaks located on the windward

wall and leaves through openings on the leeward wall. Both stack effect and wind-driven pressures are factors changing as wind speed, wind direction, and outdoor temperatures vary over time.

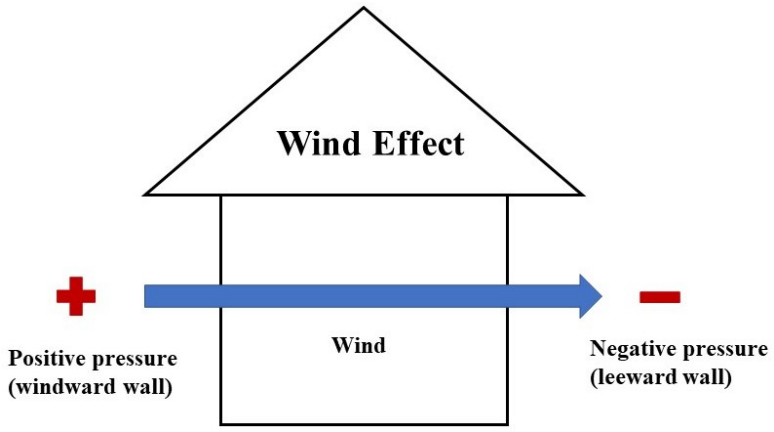

Figure 1.2: Wind effect induced by wind-driven pressures.

Mechanical ventilation system operation is the third driving force of infiltration that should be ascertained, as shown in Figure 1.3 [8]. During the operation of mechanical ventilation systems, the zone is depressurized since the indoor air is sucked out through the return fan or exhaust fan. Meanwhile, a positive pressure is created by supplying the air into the zone through the supply fan of an air handling unit (AHU). Thus, the mechanical ventilation system may pressurize or depressurize the building during the actual operational periods. It is also worth noting that with the influence of a mechanical ventilation system, the amount of infiltration during the building occupied hours is different from that during unoccupied hours.

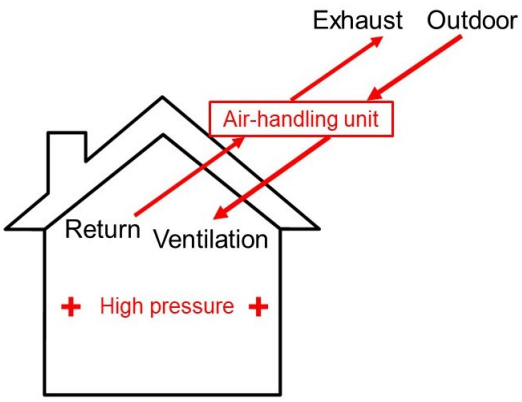

Figure 1.3: Mechanical ventilation system [8].

Despite infiltration, the distinction between ventilation and infiltration is also worth highlighting. The difference between ventilation and infiltration is the way that air flows enter the building. Unlike infiltration, ventilation refers to the airflow movement through intentional openings (e.g., ducts, windows, vents). Natural ventilation relies on the pressure difference between indoor and outdoor caused by wind and temperature difference. Mechanical ventilation is driven by the mechanical ventilation system that induces the outdoor air to be indoor and circulates indoor air at a controlled rate by using fans.

The metric of infiltration used in this thesis is air change rate. The air change rate is a metric used to describe the total rate of both building ventilation and infiltration. It represents the normalized air volume entered or removed from the test space in one hour, which is described as air changes per hour (ACH) or h^{-1}.

1.1.2 Measurement techniques

In order to monitor the impact of infiltration on buildings, various measuring techniques have been developed in the past decades. The two most common methods suggested for infiltration measurement are the tracer gas tests and standard fan pressurization tests.

Tracer gas tests described in ASTM E741 [9], including concentration decay method, constant injection method, and constant concentration method, allow experimenters to directly measure the infiltration rates by using different tracer gases (e.g., sulphur hexafluoride (SF_6), CO_2, perfluorocarbon tracer gases (PFTs)) when the mechanical ventilation system is shut down. With the mechanical ventilation system in operation, tracer gas tests can measure the total air change rate of the target zone. The concentration decay method requires injecting the tracer gas into a vacuum zone and analyze the exponential decay curve of the tracer gas concentration to obtain air change rates. The constant injection method needs a uniform injection with a constant rate to ensure the uniformity of indoor tracer gas concentration. The air change flow can be calculated based on the time series concentration measurements. The constant concentration method demands maintaining the zonal tracer gas at a constant concentration and measuring the tracer gas concentration at a fixed sampling interval. The ratio of the additional tracer gas to the desired concentration represents the average air change flow [9]. Taken from [10], Figure 1.4 illustrates the experimental set-up for tracer gas tests, including a tracer gas bottle used to dose a certain tracer gas into the test zone, a mass flow controller used to control the flow rate of dosing, a CO_2 analyzer used to quantify CO_2 concentration, an anemometer to measure the wind speed and a temperature sensor. The aforementioned tracer gas measuring techniques rely on various instrumentation, such as tracer gas injection devices, metering devices, and sampling devices. In order to ensure the smooth progress of tracer gas tests, the experimenter must be trained and familiar with all principles and the operation of the instrument.

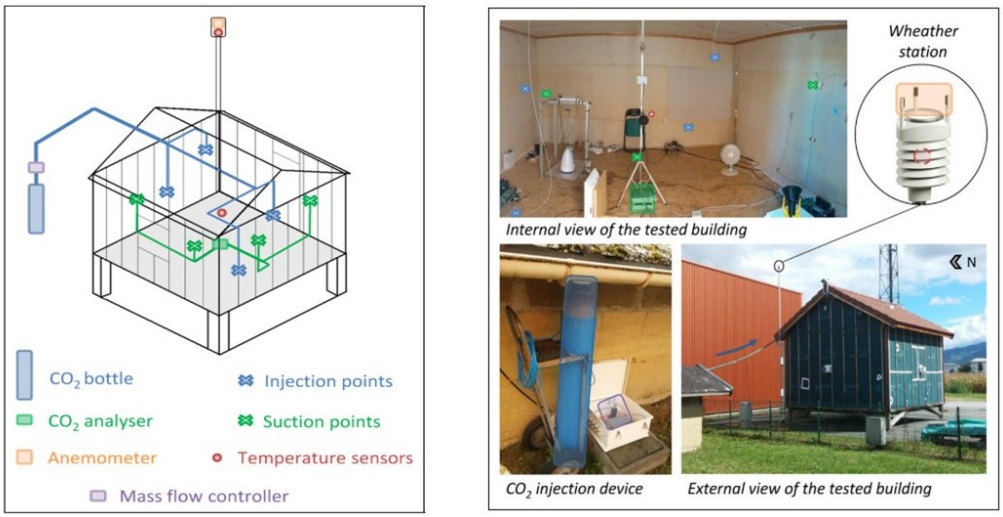

Figure 1.4: Experimental setup for tracer gas tests [10].

The standard fan pressurization test introduced in ASTM E779 [11], also known as the blower door test, is intended to characterize the airtightness of buildings. This approach measures the air leakage rates of building components rather than directly estimating building infiltration. This approach needs to pressurize or de-pressurize a single enclose zone to create a significant pressure difference (usually for 50 or 75 Pa) between indoor and outdoor by using blowers or air ducts. Then the airflow rates are measured at each sampling location and converted to air leakage rates [11]. Figure 1.5 taken from [10] exhibits the sealed door and installed fan used to deliver or suck air into or out of the test space. Similar to tracer gas, the standard fan pressurization test requires various experimental instrumentation and trained technicians.

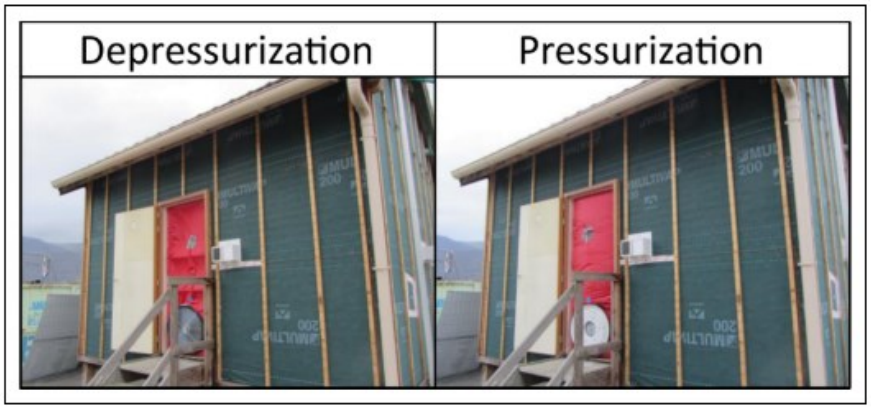

Figure 1.5: Blower door test [10].

Although tracer gas tests and fan pressurization tests have been proven to be effective for infiltration estimation and have been widely used in field studies, there are still several challenges that limit their applications to commercial buildings. First, these two methods are difficult to be employed in a large commercial building since they are intended to obtain measurements of a single zone. Second, these two methods are labour-intensive since they need various instrumentation and trained technicians to take care of the tests. Third, they have critical requirements of the experimental environment (e.g., well-mixed indoor air, uniform indoor pressure) to achieve the best precisions, which is challenging to be achieved in commercial buildings. Fourth, the side effects of conventional tests, such as the noise during equipment operation and the odour of tracer gas, may interrupt occupants' daily activities in commercial buildings.

Therefore, a low-cost and practical approach is required to monitor infiltration rates of commercial buildings. With the application of sensors inherent in BASs in commercial buildings in recent years, the CO_2 and relative humidity (RH) data are easier to collect and extract through BASs. During the unoccupied hours, the decay of residual indoor CO_2 concentration and RH (which are generated by building occupants during occupied hours) can represent an untapped

opportunity to estimate infiltration rates in a low-cost, continuous, and non-invasive fashion. Specifically, after a mechanical ventilation system is shut down and the effects of ventilation have been avoided, the decay of indoor CO_2 and RH is caused by the infiltration through building leaks. Thus, the indoor occupant-generated CO_2 and RH concentration are potential tracer gases that can be used to estimate building infiltration rates. Note that the adsorptive and desorptive effects of indoor hygroscopic materials cause decay of indoor humidity levels as well, which were discussed in detail in Chapter 2.

1.2 Research objectives and questions

Based on the environmental impact and the inadequacies of conventional infiltration testing methods, the objective of this research is to propose a low-cost inverse model-based approach to estimate infiltration rates in commercial buildings by using CO_2 and RH data extracted from the BAS. To this end, four main research questions are aimed to be presented with case studies in this integrated thesis:

- Research Question 1: Can high-cost and high-environmental impact tracer gases such as SF_6 be replaced with CO_2 in tracer gas testing?
- Research Question 2: Can BAS-grade CO_2 sensors be used instead of high accuracy CO_2 data loggers to estimate infiltration rates?
- Research Question 3: Can the humidity ratio (calculated by RH sensor data) be used in lieu of CO_2 to estimate infiltration rates as a potential tracer gas?
- Research Question 4: Can an inverse model-based approach estimate infiltration rates from historical CO_2 and humidity trend data treating occupant-generated CO_2 and moisture as the source of the tracer gas instead of dosing a specific tracer gas?

1.3 Document structure

This integrated thesis is composted of five chapters, including three (Chapters 2 - 4) which focus on the mathematical model of the proposed approach, the tracer concentration decay tests, and the case studies in detail. An introduction and conclusion chapter are also included (Chapters 1 and 5, respectively). A summary of Chapters 2 - 4 are provided below:

Chapter 2 (Laboratory experiment): This chapter details the laboratory tracer gas concentration decay tests conducted in collaboration with the National Research Council of Canada (NRC). The tracer gas tests were conducted in the Indoor Air Research Laboratory (IARL) facility located at the main campus of NRC in Ottawa, Canada. In this experiment, the SF_6 and CO_2 were injected simultaneously at five sampling locations through an injection system. Ceiling fans were used to ensure the uniformity of the indoor air mixture. A photoacoustic gas monitor was used to measure the concentration of SF_6, and CO_2 collected at the center of each sampling location. CO_2 sensors integrated with BAS also provided the CO_2 measurements.

The two independent sample t-test was chosen to verify the feasibility of replacing SF_6 with CO_2 for tracer gas concentration decay tests and the appropriateness of using BAS-integrated sensors rather than the photoacoustic gas monitor. The influence of different building pressurizations and leakage locations on air change rates was also investigated in Chapter 2. Note that the mechanical ventilation system was not shut down during this experiment; thus, the results represent the total air change rates, including ventilation rates, and infiltration rates.

Chapter 3 (Field study): This chapter presents the linear regression model used to calculate infiltration rates and compare infiltration estimates using tracer gas testing data and BAS-grade sensing data. The tracer gas tests were conducted in three private offices in an academic office building in Ottawa, Canada. The indoor air was humidified to increase the RH level, and

the CO_2 was injected into three private offices simultaneously to raise the indoor CO_2 concentration. Standalone data loggers and pre-installed BAS sensors were utilized to collect measurements in each office. Furthermore, the historical CO_2 and RH data were extracted to verify whether this model is applicable to filter out average infiltration rates of the same office from naturally occurring CO_2 and RH data. The potential reasons that affect modelling results and the pre-requisites of employing the proposed approach are discussed.

Chapter 4 (Case study): This chapter introduces average infiltration estimates of three government office buildings in Ottawa. In this chapter, two years' worth of historical CO_2 data measured by the return-air CO_2 sensors were gained from BASs to train the linear regression model. The estimates on this basis represent the system-level infiltration rates of the building. Aside from the linear regression mentioned in Chapter 2, a multiple linear regression model has been used to gain insights into the effect of wind speed and indoor/outdoor temperature difference on the proposed approach.

Chapter 2 - An inquiry into the replicability of SF_6 with CO_2 in tracer gas testing

2.1 Introduction

Two popular methods to estimate the airtightness of a building are the tracer gas (e.g., ASTM E741 [9]) and the fan pressurization (e.g., ASTM E779 [11]) tests. While fan pressurization tests are straightforward to use in the residential sector, challenges to attain a uniform differential air pressure with multiple fans make tracer gas tests far more appropriate for large commercial and institutional buildings. In terms of the accuracy and ease of application, the tracer gas tests are the preferred approach for measuring air change rates in commercial and institutional buildings.

In ASTM E741 [9], three types of standard tracer gas tests are presented: concentration decay, constant injection, and constant concentration tests. A tracer gas concentration decay test is carried out by injecting a tracer gas into an enclosed space and then stopping the injection after the test shows that the indoor concentration of the tracer gas is significantly greater than the outdoor concentration. The air change rates are then calculated from the exponential decay of the tracer gas concentration over time. For a constant injection tracer gas test, a tracer gas is injected into a test space at a constant rate. The steady-state differences between indoor and outdoor tracer gas concentrations sustained at this constant injection rate are then used to calculate the air change rates. For a constant concentration tracer gas test, the air change rate is estimated while injecting a tracer gas to maintain a constant indoor tracer gas concentration setpoint throughout the experiment. Among these approaches, the concentration decay tracer gas test is the most straightforward to employ, as it does not require a control apparatus to regulate a constant injection rate or a constant tracer gas concentration. However, the ability to estimate air exchange rates with

all three approaches is dependant on achieving a uniform distribution of the tracer gas in the test environment, an appropriate tracer gas, and an accurate monitoring device.

The selection of ideal tracer gas is related to the accuracy of the tracer gas test as well as the safety of technicians. Sherman [12] summarized several requirements for an ideal tracer gas. An ideal tracer gas must be safe (i.e., it should be non-toxic, non-allergenic, non-flammable), non-reactive (i.e., it should not react with anything during the experiment), insensible (i.e., it should not be sensible to air so as not to affect natural airflow), unique (i.e., it should be easily discriminable in the mixed air), and measurable (i.e., it should be quantifiable by measurement devices) [12].

Although the requirements for ideal tracer gas have been defined, there is no tracer gas meeting the expectations perfectly. In the past decades, various types of tracer gases have been used and compared in the field. Giesbrecht et al. [13] used water vapour as a tracer gas to estimate ventilation rates and concluded that the water vapour could be used when the building does not have high absorptive components or furnishings. Marley [14] used hydrogen (H_2), but it was difficult to be distinguished from background air.

Collins and Smith [15] used a radioactive tracer gas, argon isotope (^{41}Ar), and found that the results were in good agreement with the results acquired using H_2 as the tracer gas. Howland et al. [16] experimented with a house to measure the air movement using Krypton-85 (^{85}Kr). They summarized that using ^{85}Kr was relatively inexpensive and accurate, and it had a quicker response to the detector. Samer et al. [17] also chose ^{85}Kr as a tracer gas for the ventilation measurements in a livestock building, in which natural ventilation was applied. The results showed that the ^{85}Kr could be used to estimate air change rates in naturally ventilated buildings. Although radioactive

tracer gases are still in use today, they are expensive and complicated to obtain compared with other tracer gases [18].

To investigate the impact of tracer gas density on tracer gas test, Grimsrud [19] conducted concentration decay tests to compare the air change rates measured by using sulphur hexafluoride (SF_6), nitrous oxide (N_2O), ethane (C_2H_6), and methane (CH_4). The results showed an insignificant difference between them. In recent years, SF_6 is still one of the first-choice tracer gases when conducting tracer gas tests. Hori and Mizoguchi [20] compared the ventilation rates measured by SF_6 and isobutene, and the results were in good agreement with each other. Yoshino [21] measured ventilation rates in 39 houses by using the constant concentration method with SF_6. However, compared with other commonly used tracer gases, SF_6 traps more heat than CO_2 and has the highest global warming potential (23900 GWP).

Considering the environmental impacts and the cost of previously listed tracer gases, CO_2 is another potential choice. Cui et al. [18] presented the benefits of using CO_2 as a tracer gas: (1) its density is similar to air which makes it less likely for stratification; (2) it is safe at low concentrations; (3) it can be easily measured due to the popularity of CO_2 sensors. They also conducted a laboratory concentration decay test using CO_2 to estimate the air change rates and suggested using a multi-point sampling method to improve accuracy.

To analyze the appropriateness of applying a rule-of-thumb in dwellings, Keig et al. [22] carried out fan pressurization tests and CO_2 concentration decay tracer gas tests in four houses located in Northern Ireland. The rule-of-thumb is used to estimate annual infiltration rates at 50 Pa pressure difference by pressurizing a building in the U.K. It was defined by dividing N_{50} (the air changes per hour at 50 Pa pressure difference) by 20. Therefore, the fan pressurization test data were applied to the rule-of-thumb to estimate the infiltration flow rates. The average air change

rates were computed by the CO_2 concentration decay test. By referring to the CO_2 concentration decay tracer gas test results, the authors concluded that the rule-of-thumb overestimated the natural ventilation rates.

Carrilho et al. [23] proposed a dynamic model based on outdoor daily periodically varying CO_2 concentration to continuously estimate air exchange rates when there is no source of CO_2 in buildings. This method was also validated with the occupant-generated CO_2 concentration decay method in an apartment. After turning off the mechanical ventilation system, two data loggers were placed in the living room and balcony to monitor the variation of CO_2 concentration, which were applied to the model. By comparing the modelling results and tracer gas test estimates, the results showed that the two methods did not have a significant difference. Thebault and Millet [10] compared the air change rate estimates through a CO_2-based constant injection tracer gas test and a simplified aeraulic model introduced by a European standard EN15242. The modelling results showed that the EN15242 model tended to overestimate airflow rates.

To investigate the appropriateness of CO_2 and SF_6, several studies have been conducted. Mai et al. [24] studied the viability of estimating airflow characteristics with CO_2-based tracer gas measurements. An SF_6-based constant concentration test was also conducted to verify the results. The air change rates estimated with SF_6 and CO_2 were in good agreement. Men, Wang and Zou [25] compared the air change rates estimated through SF_6-based tracer gas decay tests to CO_2-based tracer gas constant injection tests and concluded that the difference between the results was, in general, less than 10%. SF_6 and CO_2 are both widely used tracer gases. Though, SF_6 is relatively more expensive, more difficult to obtain, and has a more significant impact on the environment than CO_2.

Although the examples mentioned above make comparisons between CO_2 and SF_6, they were all conducted in small test spaces replicating residential buildings rather than large commercial buildings. Further, essential factors, including the sensor quality, building pressurization, and air leakage locations, have not been systematically investigated. To this end, Chapter 2 presents the results from a systematic set of experiments comparing CO_2 and SF_6-based tracer gas tests to answer the following specific research questions:

Research question 2-1: Can high-cost and high-environmental impact tracer gases such as SF_6 be replaced with CO_2 in tracer gas tests?

Research question 2-2: Can BAS-grade CO_2 sensors be used instead of high-accuracy CO_2 data loggers to estimate infiltration rates?

Research question 2-3: Does the difference between CO_2 and SF_6-based tracer gas tests remain consistent at different pressurization levels?

Research question 2-4: Does the difference between CO_2 and SF_6-based tracer gas tests remain consistent when the air leakage locations are altered?

2.2 Methodology

With the aim of studying the effect of different tracer gases, sensor quality, pressurization, and leakage locations on tracer gas test results, laboratory tracer gas tests with SF_6 and CO_2 were carried out, and the details are introduced in this section.

2.2.1 Indoor Air Research Laboratory (IARL)

The tracer gas tests were conducted in the Indoor Air Research Laboratory (IARL), which is located at the National Research Council of Canada (NRC) campus in Ottawa, Canada. Figure 2.1 shows the structure of the IARL that consists of two storeys, a basement, and a garage. This

research facility was constructed with 418 m^2 total floor area. Figure 2.2 exhibits schematics of the ground floor, second floor and the basement of IARL.

Figure 2.1: Indoor air research laboratory (IARL).

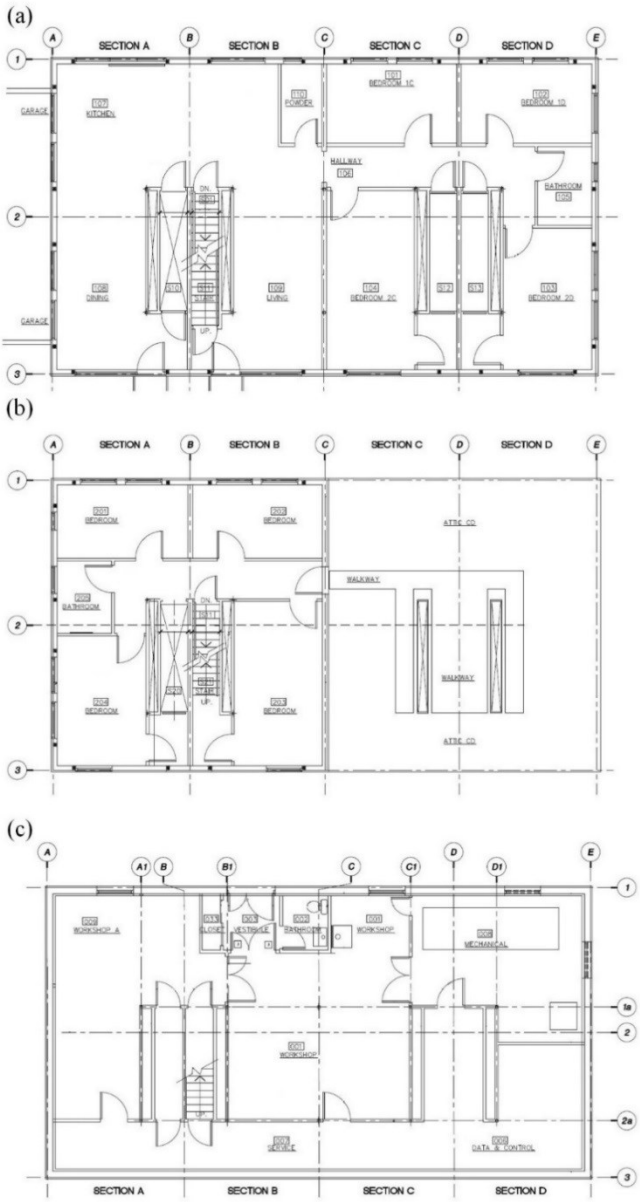

Figure 2.2: Floor plan of (a) ground floor, (b) second floor, and (c) basement.

2.2.1.1 Mechanical system

The IARL has one air handling unit (AHU), which is located in the basement and is highlighted in Figure 2.3. The AHU was dedicated to maintaining the desired building pressures. Each supply and return duct leading to each room has a motorized damper to completely control the airflow rates to and from the room. The building automation system (BAS) of this facility controls the operation of AHU and contains CO_2 sensors to measure the variation of indoor CO_2 concentration.

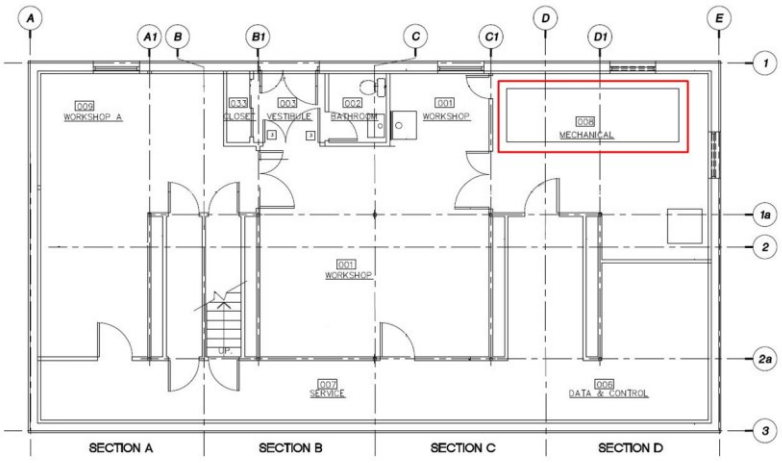

Figure 2.3: IARL AHU location.

There are also 31 envelope ports built-in to the IARL, and each envelope port is installed with a motorized damper that can be controlled by the BAS to simulate different leakage locations. In order to test different air leakage arrangements, five envelope ports of the IARL were selected. Figure 2.4 labels the selected envelope ports (d1, d2, d3, d4 and d5).

Figure 2.4: Five envelope ports were used in experiments. Note that "d" represents the damper in each envelope port.

Figure 2.5 (a), (b) and (c) show the sampling locations, sensor locations, ceiling fan locations, as well as the locations of five selected envelope ports. The figure indicates the SF_6 and CO_2 measurement locations in the test facility. The term "PHOTO" in the figure represents the photoacoustic gas monitors used in the facility. The CO_2 concentration was also measured by BAS-grade sensors pre-installed on the walls of each location to verify if CO_2 BAS-grade sensors were applicable for estimating air change rates in lieu of using high accuracy measurement devices.

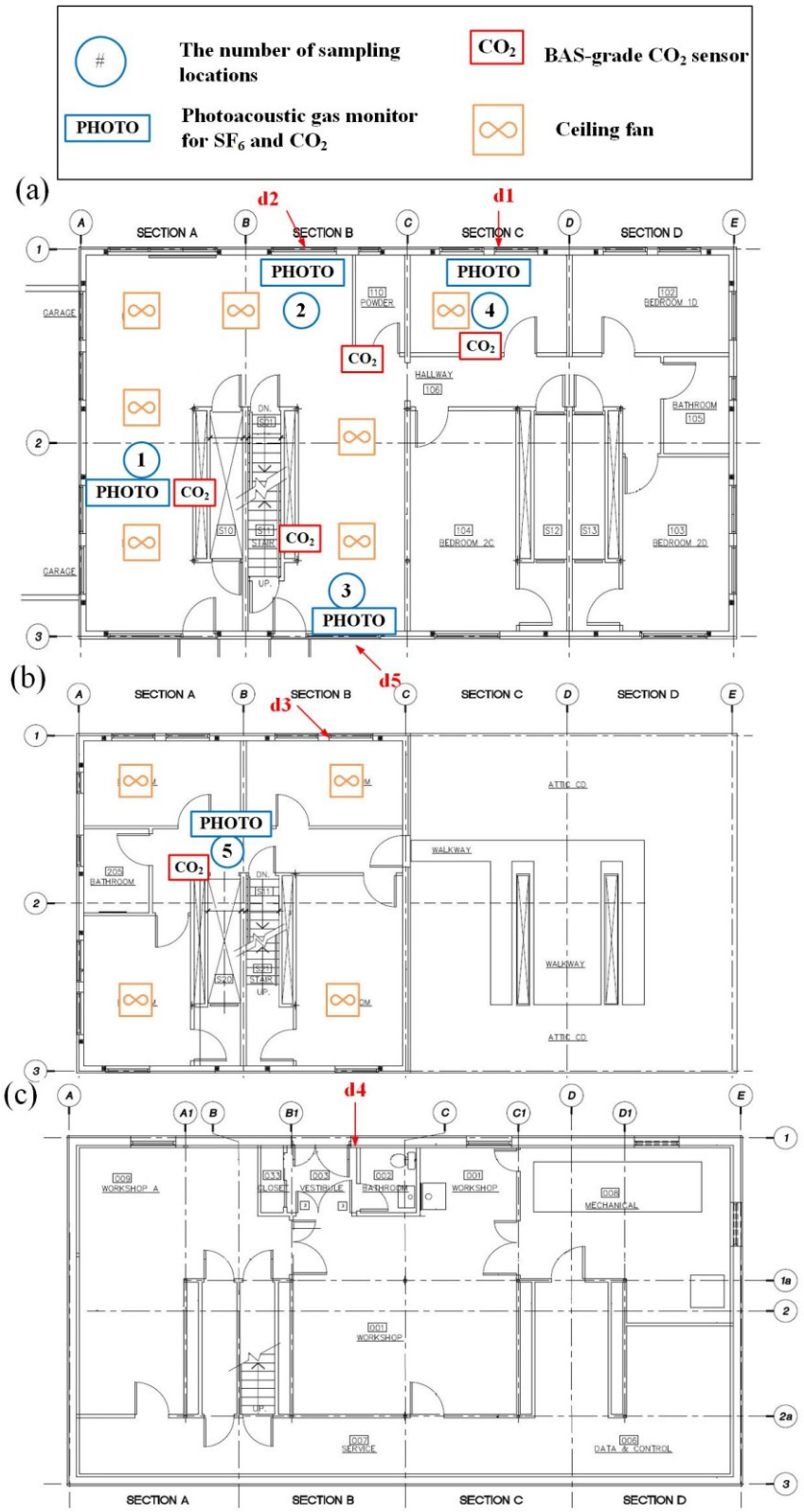

Figure 2.5: (a) The ground,(b) second, and (c) basement floor plan labelled with sampling locations, BAS-grade CO_2 sensor locations, ceiling fan locations, and envelope ports.

2.2.1.3 Tracer gas system

The tracer gas tests were conducted through the tracer gas system pre-constructed in the IARL. The tracer gas system consists of three main components, including an injection system, a sampling system, and measuring devices. Figure 2.6 shows the dosing location and the mass flow controller that allows injecting tracer gases into the return duct of the AHU at a constant rate. The mechanical ventilation system in the IARL is responsible for delivering tracer gases through the building for measurement at various sampling locations.

Figure 2.6: Mass flow controller and dosing location.

The sampling system is detailed in Figure 2.7. A photoacoustic gas monitor (INNOVA 1512-5 photoacoustic gas monitor) in conjunction with two 1409-24 multiplexers and sampling lines allow measuring the tracer gas concentrations at different sampling locations simultaneously. Each sampling line is used to extract the mixing air at the center of each sampling location, while the pump in each sampling line helps transport sampled air to the photoacoustic gas monitor and return it to sampling locations. A ventilation measurement application software (7650 Basic

Ventilation Software) was used to remotely control the dosing system and photoacoustic gas monitor and acquire the measurements of sampled air collected from each sampling location.

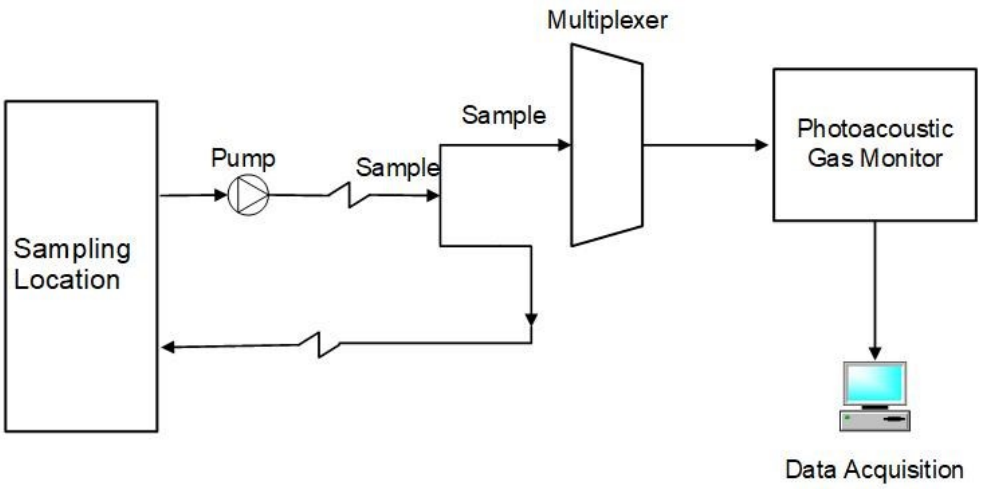

Figure 2.7: Schematic diagram of a multi-position tracer gas sampling system.

In this study, the CO_2 and SF_6 were dosed simultaneously into the return duct of the AHU by the injection system, and they were dispatched into the entire building by a mechanical ventilation system. Then tracer gases mixed sufficiently with indoor air through the support of ceiling fans. The air samples were captured from the center of five sampling locations through the sampling system and measured by the photoacoustic gas monitor. During this time, the variation of indoor CO_2 concentration was also measured by BAS-grade CO_2 sensors.

2.2.2 Experiment program

2.2.2.1 Experimental scenarios

Different combinations of dampers installed in selected envelope ports allow to test the air change rates when the air leakage locations are on the same wall (d1 and d2 are open), across the room (d2 and d5 are open), and on the same side but at a different height (d3 and d4 open). Moreover, the tracer gas tests are conducted separately under two different positive pressures (i.e.,

10 and 15 Pa) induced and maintained by the AHU, which the BAS controlled. There were five experimental scenarios examined in this study, as listed in Table 2.1. The comparison between experiments 1 and 3, and experiments 2 and 4 reveal whether the differences between SF_6 and CO_2-based tracer gas tests remain consistent at different pressurization levels, while the comparison between experiments 3, 4 and 5 demonstrates the impact of different leakage locations on the tracer gas test.

Table 2.1: Experimental scenarios in the recent study.

Experiment	Pressure (Pa)	Open Dampers	Runs
1	10	d1 and d2	4
2	10	d2 and d5	4
3	15	d1 and d2	5
4	15	d2 and d5	6
5	15	d3 and d4	6

At the beginning of each experiment, the injection system was designed to inject SF_6 and CO_2, allowing the tracer gas concentration to increase significantly and reach a peak value in one hour. Then the injection system was shut down over the next seven hours to ensure the tracer gas concentration decayed to the outdoor level. The injection system was also programmed to re-dose when the seven-hour decay phase finished, and different repeated runs were performed for each scenario. Note that tracer gas concentrations obtained at five sampling locations were all measured simultaneously during each experiment. For experiment 1, the tracer gas tests were repeated four times, meaning that the variation of SF_6 and CO_2 were repeatedly measured four times at five sampling locations. Similar to experiment 1, the repeated concentration decay tracer gas tests were conducted four times, five times, six times and six times for experiments 2, 3, 4, and 5, respectively.

2.2.2.2 Data preprocessing and analysis

The following differential equation defines the decay phase of tracer gas concentration:

$$\frac{dC}{dt} = (C_t - C_{oa}) \cdot \frac{q}{V} \quad (2.1)$$

where C_t is the indoor time-varying concentration of tracer gas in the decay phase, C_{oa} is the outdoor tracer gas concentration, q is the airflow rate in m^3/s and V is the volume of the single test zone in m^3. With the intention of accounting for the bias in each sensor, the differences between the minimum recorded tracer gas concentration and the outdoor concentration (e.g., 0 ppm for SF_6 and 400 ppm for CO_2) were removed [28–30].

Eqn. 2.2 is obtained by solving Eqn. 2.1 with the first-order forward difference approximation:

$$C_{t+\Delta t} - C_t = (C_t - C_{oa}) \cdot (\frac{q}{V} \cdot \Delta t) \quad (2.2)$$

where $C_{t+\Delta t} - C_t$ indicates the difference of tracer gas concentration between adjacent time steps, and $C_t - C_{oa}$ is the difference of tracer gas concentration between indoor and outdoor at time t. Note that the $\frac{q}{V} \cdot \Delta t$ represents the air changes per hour (h^{-1}) using a one-hour time step in this study. Recall that air change rate equals the airflow divided by the volume of the test zone and is usually described in air changes per hour [29].

The two independent sample t-tests were used to determine whether the mean of one group is different from the other group. The following equation defines the *t-value* [30], which is used to indicate whether a statistically significant difference exists within a dataset:

$$t - value = \frac{\overline{X}_1 - \overline{X}_2}{\frac{(n_1-1)\cdot {S_1}^2 + (n_2-1)\cdot {S_2}^2}{n_1+n_2-2} * \sqrt{\frac{1}{n_1} + \frac{1}{n_2}}} \quad (2.3)$$

where $\overline{X}_1$ and $\overline{X}_2$ are the mean values, S_1 and S_2 are variance, and n_1 and n_2 are the sample size of each group (i.e., the number of data points in each sample set).

To investigate the significant level of calculated *t-value*, the degrees of freedom (*d.f.*) and the corresponding critical *t-value* (t_{cri}) of the t-test selected from the statistical table (i.e., the critical value of Student t-distribution) are applied. The *d.f.* depends on the sample size, which equals $n_1 + n_2 - 2$. Thus, the t_{cri} is selected from the *t* table according to the value of *d.f.* and the confidence level that depends on the pre-selected statistical significance level (i.e., the α value) [30].

With reporting *t-value*, t_{cri}, and *d.f.*, the larger *t-value* represents a higher possibility that the significant difference exists between the two groups, whereas the smaller *t-value* represents the two groups are more similar to each other. Once the calculated *t-value* is greater than t_{cri} and the p-value is less than the significance level, the null hypothesis should be rejected as this situation indicating that the mean value of one group is significantly different from the other group.

In this study, the two independent sample t-tests compared the mean difference between air change rates estimated from SF_6 and those estimated from CO_2 data measured by the photoacoustic gas monitor (hereafter will be abbreviated as SF_6 photoacoustic air change rates and CO_2 photoacoustic air change rates) to find out whether the tracer gas types have an impact on air change rates (research question 2-1). Similarly, to investigate the effect of sensor quality (research question 2-2), the two independent sample t-tests were also used to determine the mean difference between CO_2 photoacoustic air change rates and the air change rates estimated from CO_2 data measured by BAS sensors (hereafter will be abbreviated as CO_2 BAS air change rates). The two independent sample t-tests were tested at the 0.05 level of significance ($\alpha = 0.05$) in this study.

2.3 Results and Discussion

This section presents the air change rates estimated based on SF_6 and CO_2 concentration measured by the concentration decay method and the results of two independent sample t-tests.

2.3.1 Air change rates

Figure 2.8 shows the air change rates calculated based on the tracer gas concentration measured from sampling location 1. The values annotated at the top of each group represent the average air change rate calculated from the air change rates measured by repeated experimental runs. For instance, in Figure 2.8 (a), the average SF_6 and CO_2 photoacoustic air change rate, as well as average CO_2 BAS air change rate, are 1.04 h^{-1}, 1.06 h^{-1}, and 1.01 h^{-1}, respectively. Most of the deviation of average air change rates in Figure 2.8 is less than 10%. The highest deviation of the average air change rate between SF_6 (1.23 h^{-1}) and CO_2 (1.38 h^{-1}) photoacoustic air change rates is -12% at sampling location 1 for Experiment 3 (Figure 2.8 (c)), which represents the average air change rate calculated from CO_2 photoacoustic sensor measurements is 12% higher than SF_6-based one.

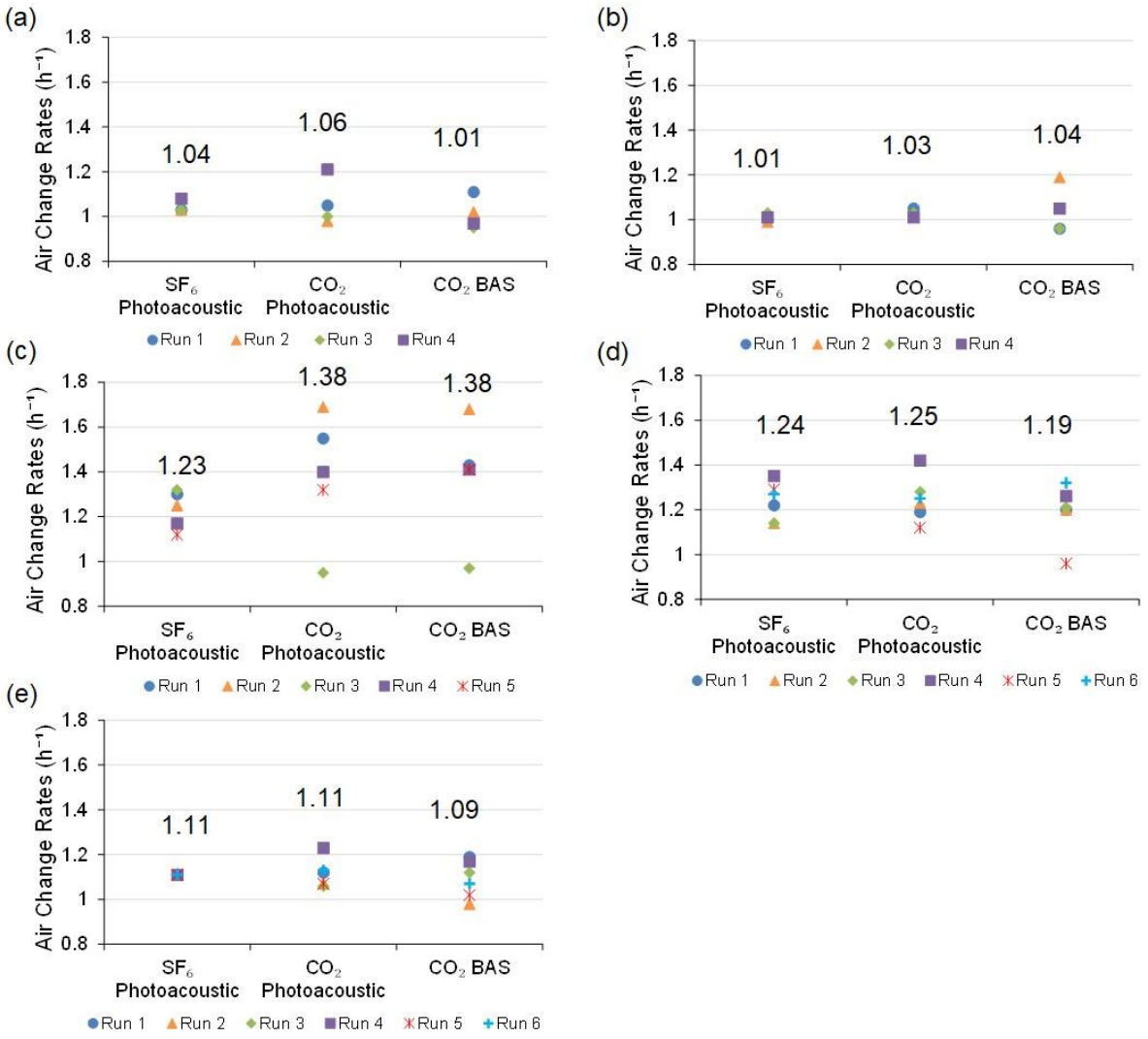

Figure 2.8: Air change rates calculated from sampling location 1 for experiments (a) 1, (b) 2, (c) 3, (d) 4, and (e) 5. The numbers annotated above the scatter points are the mean of each group.

Figure 2.9 illustrates air change rates measured from sampling location 2. The overview of comparisons between average SF_6 and CO_2 photoacoustic air change rates indicates that using CO_2 as tracer gas usually overestimates the air change rates. However, the deviations were less than 10%. For the analysis of sensor quality, Experiment 3 (Figure 2.9 (c)) deviates the most, where the average CO_2 BAS air change rate (1.18 h^{-1}) is 12% less than CO_2 photoacoustic one (1.34 h^{-1}).

Average CO_2 BAS air change rates estimated from Experiments 4 and 5 are slightly less than CO_2 photoacoustic results with a deviation of around 4%.

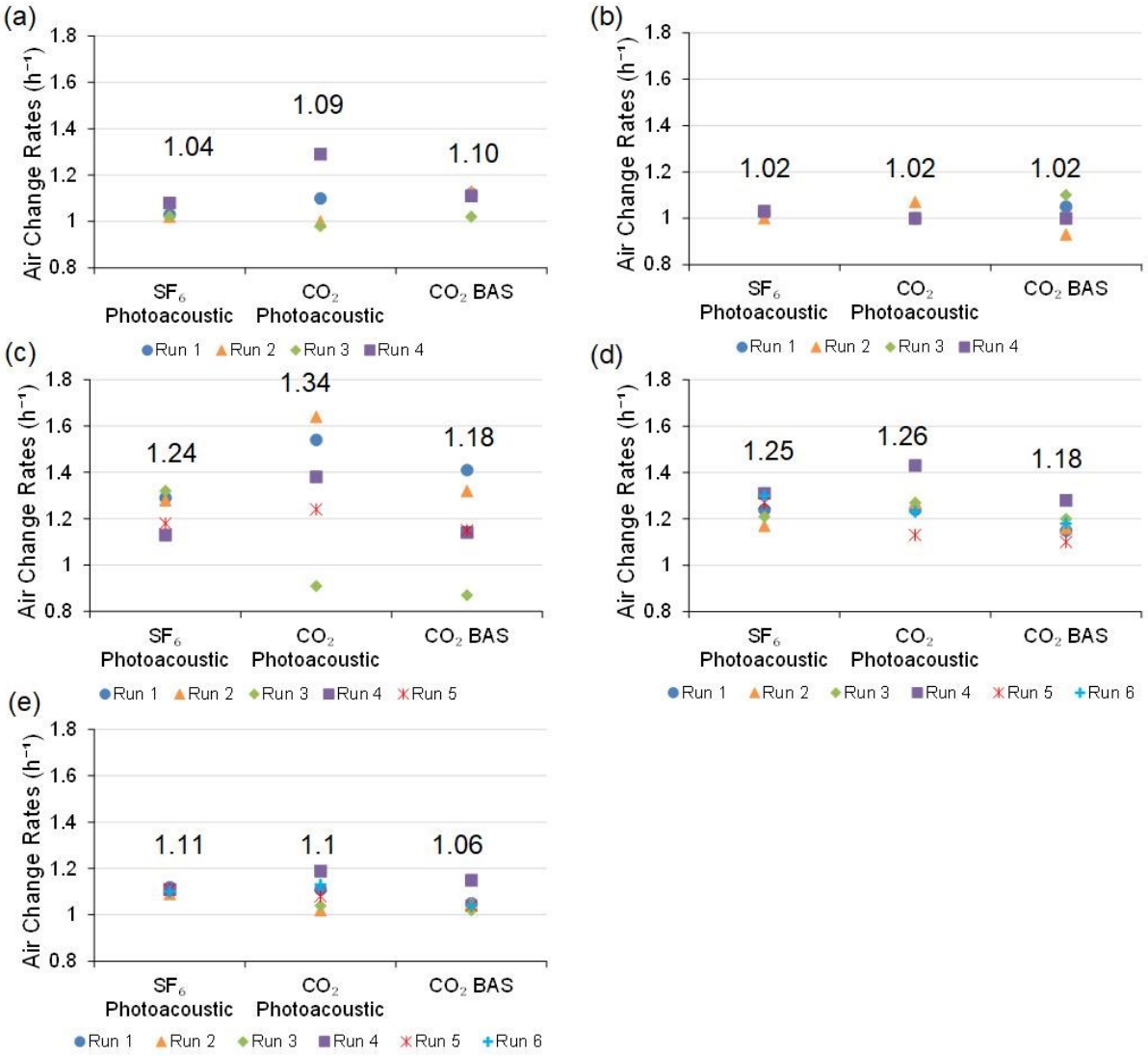

Figure 2.9: Air change rates calculated from sampling location 2 for experiments (a) 1, (b) 2, (c) 3, (d) 4, and (e) 5. The numbers annotated above the scatter points are the mean of each group.

For air change rates measured from sampling location 3, the sensor quality-based analysis is highlighted. As shown in Figure 2.10 (e), the average CO_2 BAS air change rate (0.93 h^{-1})

measured at sampling location 3 deviates the most (15%) from the average CO_2 photoacoustic air change rate (1.09 h^{-1}). The deviations of other cases at sampling location 3 were less than 10%.

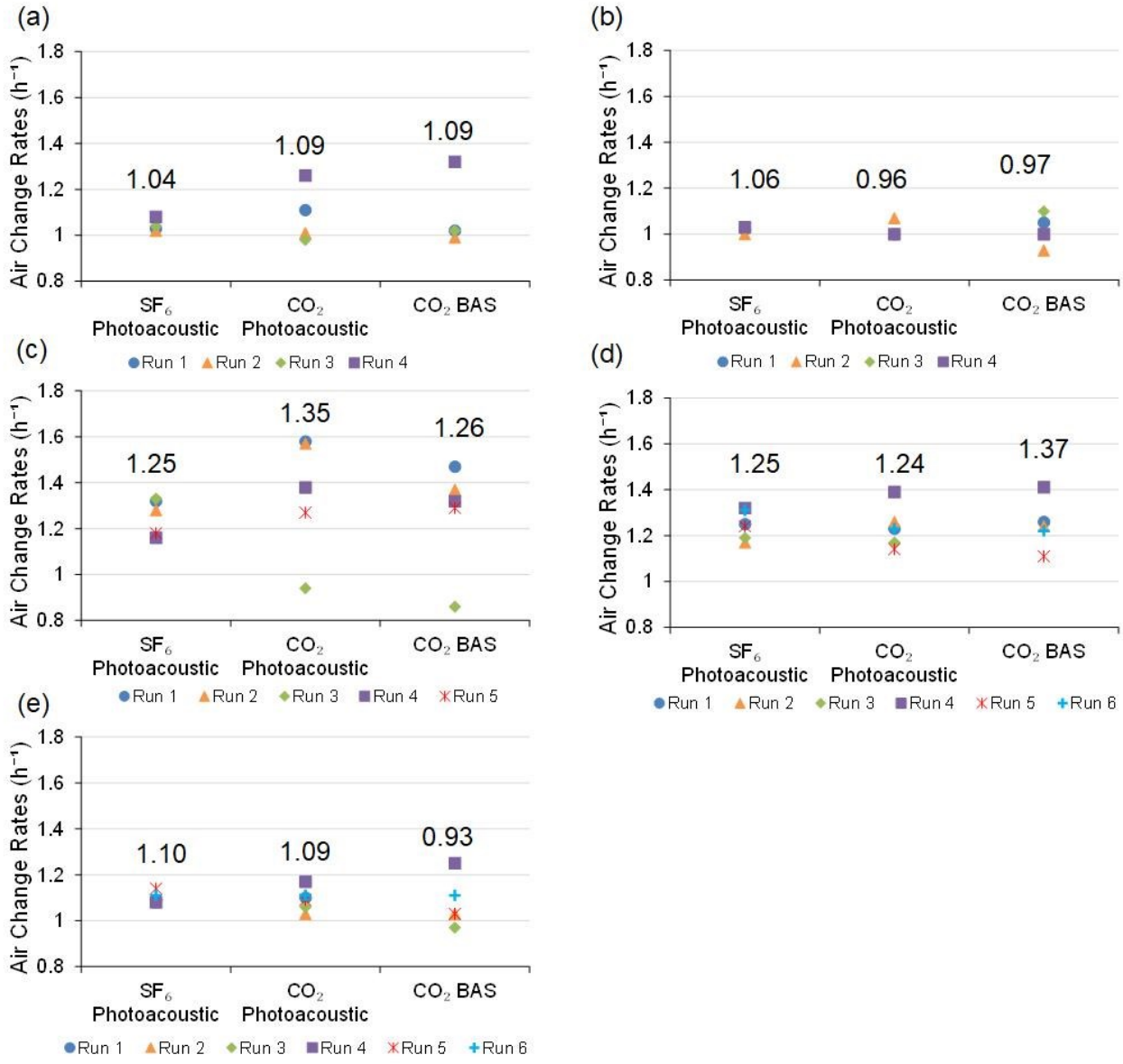

Figure 2.10: Air change rates calculated from sampling location 3 for experiments (a) 1, (b) 2, (c) 3, (d) 4, and (e) 5. The numbers annotated above the scatter points are the mean of each group.

The average air change rates of all cases displayed in Figure 2.11 and Figure 2.12 can be considered acceptable due to the comparison of tracer gases and sensor quality. The deviations

were less than 10%, with a maximum of 7% (Figure 2.11 (d)) and a minimum of 0 (Figure 2.11 (c) and Figure 2.12 (c)).

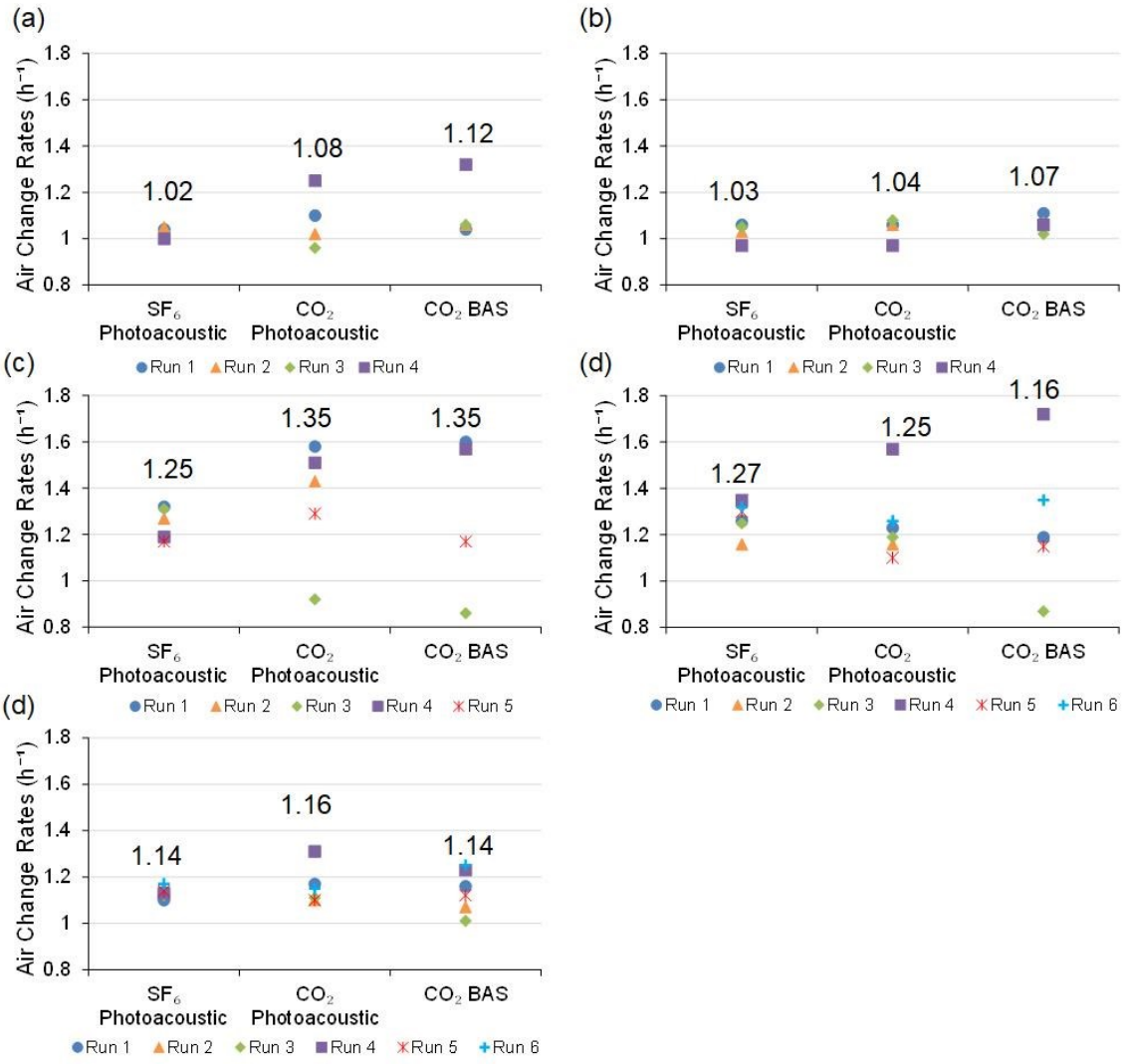

Figure 2.11: Air change rates calculated from sampling location 4 for experiments (a) 1, (b) 2, (c) 3, (d) 4, and (e) 5. The numbers annotated above the scatter points are the mean of each group.

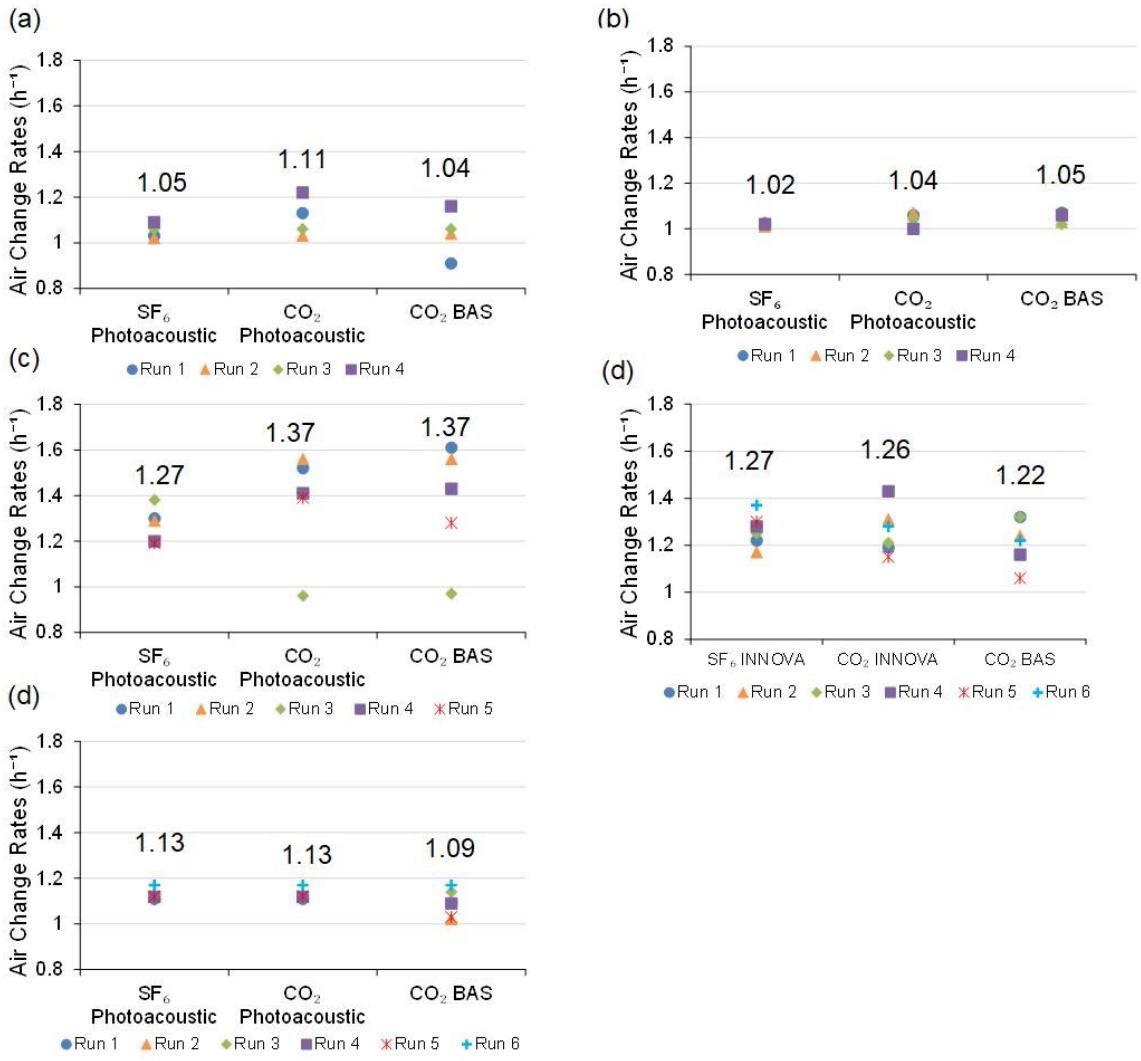

Figure 2.12: Air change rates calculated from sampling location 5 for experiments (a) 1, (b) 2, (c) 3, (d) 4, and (e) 5. The numbers annotated above the scatter points are the mean of each group.

In accordance with statistical analysis, the overview of CO_2-based air change rates, including CO_2 photoacoustic and CO_2 BAS air change rates, is larger than the SF_6 photoacoustic air change rate. Some exceptions show that the average CO_2 BAS-based air change rate sometimes stays inconsistent with CO_2 photoacoustic-based results. However, in the engineering sense, the differences between SF_6-based and CO_2-based air change rates are acceptable. The highest difference between average SF_6 and CO_2 photoacoustic air change rate, is 0.15 h^{-1} as shown in

Figure 2.8 (c), while average CO_2 photoacoustic air change rates differ the most from the average CO_2 BAS air change rate with 0.16 h^{-1}.

2.3.2 Two independent sample t-test

Table 2.2 and 2.3 tabulate the two independent sample t-tests results based on the comparison between SF_6 and CO_2 photoacoustic air change rates (i.e., the SF_6 and CO_2) and the comparison between CO_2 photoacoustic and CO_2 BAS air change rates (i.e., sensor accuracy) for experimental scenario 1 and 3. The significance level of 0.05 ($\alpha = 0.05$) was used for this analysis, and the null hypotheses tested in the two independent sample t-tests in this study are:

(1) SF_6-based air change rates are not statistically different from CO_2-based air change rates.

(2) Air change rates estimated from a low-cost CO_2 BAS sensor are not statistically different from those estimated from an expensive high-accuracy CO_2 sensor.

According to the table, *t-values* calculated from all sampling locations in both experimental scenarios are less than t_{cri} and all p-values are greater than 0.05, indicating that the aforementioned null hypotheses are retained. Specifically, there is no difference between the means calculated from the photoacoustic gas monitoring system, which represents using SF_6 or CO_2 during tracer gas concentration decay tests does not have statistically significant effects on air change rates. Similarly, the conclusion can be drawn for the second null hypothesis that CO_2 photoacoustic and CO_2 BAS air change rates are not statistically different from each other. Thus, in lieu of SF_6, the CO_2 can be used as a tracer (research question 2-1), and the low-cost BAS-grade sensor can be used to replace high accuracy data logger (research question 2-2) when employing the tracer gas concentration decay method.

Table 2.2: Two sample independent t-test results for experimental scenarios 1.

Sampling Location	Same Wall, 10 Pa							
	SF_6 and CO_2				Sensor Quality			
	t-value	t_{cri}	*p*	*d.f.*	*t-value*	t_{cri}	*p*	*d.f.*
1	0.33	1.94	0.38	6	0.75	1.94	0.24	6
2	0.76	1.94	0.24	6	0.033	1.94	0.49	6
3	0.74	1.94	0.24	6	0.025	1.94	0.49	6
4	0.94	1.94	0.19	6	0.41	1.94	0.35	6
5	1.33	1.94	0.12	6	1.01	1.94	0.17	6

Table 2.3: Two sample independent t-test results for experimental scenarios 3.

Sampling Location	Same Wall, 15 Pa							
	SF_6 and CO_2				Sensor Quality			
	t-value	t_{cri}	*p*	*d.f.*	*t-value*	t_{cri}	*p*	*d.f.*
1	1.15	1.86	0.14	8	0.012	1.86	0.5	8
2	0.77	1.86	0.23	8	0.4	1.86	0.16	8
3	0.77	1.86	0.23	8	0.55	1.86	0.3	8
4	0.78	1.86	0.23	8	0.042	1.86	0.48	8
5	0.85	1.86	0.21	8	0.013	1.86	0.5	8

Table 2.4 and 2.5 list the two independent sample t-tests results for experimental scenarios 2 and 4. Similar to experimental scenarios 1 and 3, with the exclusion of the bolded *t-value* and p-value of tracer gas type obtained in sampling location 3 in Table 2.4, the rest are less than critical values, which indicates that the CO_2 is acceptable to be applied to the proposed approach and the BAS-grade sensor is also applicable for experimental scenario 2 and 4.

Table 2.4: Two independent sample t-tests results for experimental scenarios 2.

Sampling Location	Across room, 10 Pa							
	SF_6 and CO_2				Sensor Quality			
	t-value	t_{cri}	*p*	*d.f.*	*t-value*	t_{cri}	*p*	*d.f.*
1	1.66	1.94	0.074	6	0.24	1.94	0.41	6
2	0.13	1.94	0.45	6	0.062	1.94	0.48	6
3	**12.25**	**1.94**	**0.00**	6	0.57	1.94	0.29	6

4	0.47	1.94	0.33	6	0.73	1.94	0.25	6
5	1.41	1.94	0.1	6	0.13	1.94	0.45	6

Table 2.5: Two independent sample t-tests results for experimental scenarios 4.

Sampling Location	Across room, 15 Pa							
	SF_6 and CO_2				Sensor Quality			
	t-value	t_{cri}	*p*	*d.f.*	*t-value*	t_{cri}	*p*	*d.f.*
1	0	1.81	0.5	10	0.87	1.81	0.2	10
2	0.25	1.81	0.4	10	1.79	1.81	0.52	10
3	0.23	1.81	0.41	10	1	1.81	0.17	10
4	0.3	1.81	0.39	10	0.57	1.81	0.29	10
5	0.067	1.81	0.47	10	0.72	1.51	0.24	10

The bolded *t-value* indicates the Type I error in hypothesis tests that the first null hypothesis was incorrectly rejected in this study. The probability of this Type I error is 5% ($\alpha = 0.05$), stating that it is acceptable to have a 5% chance to erroneously reject the null hypothesis given that it is true [30]. To prove the first aforementioned null hypothesis, Table 2.6 shows the detailed average infiltration rates and corresponding R^2 values of comparison between SF_6 and CO_2 photoacoustic-based analysis when the leakage locations are across the room at 10 Pa (i.e., the bolded *t-value* in Table 2.4). The most significant deviation between SF_6 photoacoustic air change rates and their average occurred in run 2, which was 1.4% lower than the average value. Run 4 deviated the most for CO_2 photoacoustic air change rates, which was 1.6% lower than the average. Moreover, the deviation between the two average air change rates is 9.4%, and the difference between them is around 0.1 h^{-1}. Therefore, although the statistical results indicate a difference between the group means (*t-value* > t_{cri}), the distinction of air change rate between SF_6 and CO_2 is acceptable in the engineering sense.

Table 2.6: The air change rates for each run at sampling location 3 in experimental scenario 2.

Run	SF_6 Photoacoustic		CO_2 Photoacoustic	
	Air Change Rate (h^{-1})	R^2	Air Change Rate (h^{-1})	R^2
1	1.07	0.98	0.96	0.97
2	1.04	0.98	0.96	0.97
3	1.06	0.98	0.96	0.97
4	1.05	0.98	0.94	0.96
Average	1.06	-	0.96	-

2.3.3 Impacts of pressurization levels and leakage locations

An overview of the average air change rates of all sampling locations is tabulated in Table 2.7 and Table 2.8 in order to investigate whether the difference between CO_2 and SF_6-based tracer gas tests remains consistent at different pressurization levels (research question 3). According to the following tables, increased building pressure leads to higher average air change rates at the same sampling location. Nevertheless, differences in results between SF_6 and CO_2 are consistent when building pressure changes. For the comparison between experiments 1 and 3, the average difference between using SF_6 and CO_2 are 0.21 h^{-1} and 0.27 h^{-1}, respectively. The highest deviation is 0.23 h^{-1} at sampling location 4 for SF_6-based results and 0.32 h^{-1} at sampling location 1 for CO_2-based results, whereas the lowest difference is 0.19 h^{-1} for SF_6-based and 0.25 h^{-1} for CO_2-based analysis. The average air change rates listed in Table 2.8 show that for experiments 2 and 4, the average difference between the two methods is the same (0.23 h^{-1}), with a maximum of 0.25 h^{-1} for SF_6-based analysis and 0.28 h^{-1} for CO_2-based analysis. Thus, the investigation revealed that the CO_2 can be used instead of SF_6 at different pressurization levels.

Table 2.7: Comparison between average SF_6 and CO_2 air change rates at different building pressures for experiments 1 and 3.

	SF_6 Photoacoustic (h^{-1})			CO_2 Photoacoustic (h^{-1})		
Sampling Locations	Same Wall, 10Pa	Same Wall, 15Pa	Diff.	Same Wall, 10Pa	Same Wall, 15Pa	Diff.
1	1.04	1.23	0.19	1.06	1.38	0.32
2	1.04	1.24	0.20	1.09	1.34	0.25
3	1.04	1.25	0.21	1.09	1.35	0.26
4	1.02	1.25	0.23	1.08	1.35	0.27
5	1.05	1.27	0.22	1.11	1.37	0.26
Avg.	-	-	0.21	-	-	0.27

Table 2.8: Comparison between average SF_6 and CO_2 air change rates at different building pressures for experiments 2 and 4.

	SF_6 Photoacoustic (h^{-1})			CO_2 Photoacoustic (h^{-1})		
Sampling Locations	Across Room, 10 Pa	Across Room, 15 Pa	Diff.	Across Room, 10 Pa	Across Room, 15 Pa	Diff.
1	1.01	1.24	0.23	1.03	1.25	0.22
2	1.02	1.25	0.23	1.02	1.23	0.21
3	1.06	1.25	0.19	0.96	1.24	0.28
4	1.03	1.27	0.24	1.04	1.25	0.21
5	1.02	1.27	0.25	1.04	1.26	0.22
Avg.	-	-	0.23	-	-	0.23

To examine whether the leakage location affects SF_6-based and CO_2-based tracer gas test results, Table 2.9 (experiments 1 and 2) and Table 2.10 (experiments 3 and 4) display the difference of average air change rates estimated at 10 Pa and 15 Pa with different locations on the ground floor. The average differences in Table 2.9 are small for both two tracer gases, which is 0.01 h^{-1} for using SF_6 and 0.07 h^{-1} for using CO_2. For Table 2.10, the results estimated based on average SF_6 photoacoustic air change rates reveal a 0.01 h^{-1} difference. However, the CO_2-based results differ comparatively more, with an average difference of 0.11 h^{-1}.

Table 2.9: Comparison between average SF_6 and CO_2 air change rates at different leakage locations for experiments 1 and 2.

	SF_6 Photoacoustic (h^{-1})			CO_2 Photoacoustic (h^{-1})		
Sampling Locations	Same Wall, 10 Pa	Across Room, 10 Pa	Diff.	Same Wall, 10 Pa	Across Room, 10 Pa	Diff.
1	1.04	1.01	0.03	1.06	1.03	0.03
2	1.04	1.02	0.02	1.09	1.02	0.07
3	1.04	1.06	0.02	1.09	0.96	0.13
4	1.02	1.03	0.01	1.08	1.04	0.04
5	1.05	1.02	0.03	1.11	1.04	0.07
Avg.	-	-	0.01	-	-	0.07

Table 2.10: Comparison between average SF_6 and CO_2 air change rates at different leakage locations for experiments 3 and 4.

	SF_6 Photoacoustic (h^{-1})			CO_2 Photoacoustic (h^{-1})		
Sampling Locations	Same Wall, 15 Pa	Across Room, 15 Pa	Diff.	Same Wall, 15 Pa	Across Room, 15 Pa	Diff.
1	1.23	1.24	0.01	1.38	1.25	0.13
2	1.24	1.25	0.01	1.34	1.23	0.11
3	1.25	1.25	0.00	1.35	1.24	0.11
4	1.25	1.27	0.02	1.35	1.25	0.10
5	1.27	1.27	0.00	1.37	1.26	0.11
Avg.	-	-	0.01	-	-	0.11

Table 2.11 tabulates the results to explore whether changing the height of leakage locations (experiments 3 and 5) affects SF_6 and CO_2-based tracer gas tests. The results listed in Table 2.11 show the acceptable difference when the leakage locations have a height difference, with 0.13 h^{-1} for SF_6-based tracer gas tests and 0.24 h^{-1} for CO_2-based tracer gas tests.

Table 2.11: Comparison between average SF_6 and CO_2 air change rates at different leakage locations for experiments 3 and 5.

	SF_6 Photoacoustic (h^{-1})			CO_2 Photoacoustic (h^{-1})		
Sampling Locations	Same Wall, 15 Pa	Different Height, 15 Pa	Diff.	Same Wall, 15 Pa	Different Height, 15 Pa	Diff.
1	1.23	1.11	0.12	1.38	1.11	0.27
2	1.24	1.11	0.13	1.34	1.10	0.24
3	1.25	1.10	0.15	1.35	1.09	0.26
4	1.25	1.14	0.11	1.35	1.16	0.19
5	1.27	1.13	0.14	1.37	1.13	0.24
Avg.	-	-	0.13	-	-	0.24

All results mentioned in this section focus on answering research questions 2-3 and 4. In accordance with most cases, two conclusions can be drawn. First, CO_2 can replace SF_6 as a tracer

gas in the tracer gas concentration decay tests if the pressure difference is low. Second, the leakage location has no obvious effect on the tracer gas test results when using CO_2.

2.3.4 Discussion

Based on the results of tracer gas concentration decay tests presented in the previous sections, the possible explanation of differences produced by the SF_6-based and CO_2-based methods is that the sampling location potentially influences the measurements collected by measurement devices. The CO_2 photoacoustic measurements were sampled at the center of the sampling location through the sampling line, whereas the CO_2 BAS-grade sensors were pre-installed on the wall. Compared with CO_2, SF_6 has a larger molecular weight that potentially settles down after dosing and causes stratification during measurement. Although they gained samples simultaneously, the nonuniformity caused by stratification is also possible to generate bias due to the spatial difference.

In terms of the specific research question 2-4 mentioned in this chapter, the comparisons shown from Table 2.7 to 2.9 reveal that the leakage location does not noticeably affect tracer gas test results. This is contrary to the conclusion of the previous study [31] that the leakage location has a statistically significant impact on air change rates. Compared with the experiments conducted by Berquist et al. [31], the tracer gas concentration decay tests in this study were only conducted in the shoulder month (May 2021), while the air change rates obtained from the previous study were based on whole-year concentration decay tests. During four seasons, varying weather conditions, for example, outdoor temperature, wind speed and wind direction, can significantly affect the infiltration, in turn, the total air change rates.

2.4 Closing remarks

The aim of Chapter 2 is to answer four specific research questions based on laboratory tracer gas concentration decay tests: (1) Can high-cost and high-environmental impact tracer gases such as SF_6 be replaced with CO_2 in tracer gas tests? (2) Can BAS-grade CO_2 sensors be used instead of high accuracy CO_2 data loggers to estimate infiltration rates? (3) Does the difference between CO_2 and SF_6-based tracer gas tests remain consistent at different pressurization levels? (4) Does the difference between CO_2 and SF_6-based tracer gas tests remain consistent when the air leakage locations are altered?

Chapter 2 introduces the laboratory tracer gas concentration decay tests at the IARL facility of NRC. During experiments, the SF_6 and CO_2 were injected into the duct and monitored at sampling locations through the mechanical ventilation system, and the tracer gas concentration was measured simultaneously by a photoacoustic gas monitor and BAS-grade sensors. The two independent sample t-test results highlight that the CO_2 can be used as a tracer gas when tracer gas concentration decay methods are employed. Also, the high accuracy data logger can be replaced with a low-cost sensor integrated with BAS in tracer gas tests. By comparing the average air change rates estimated at different pressure and leakage levels, it is clear that CO_2 is applicable in tracer gas tests, with the differences between SF_6 and CO_2-based methods consistent as building pressure changes and leakage locations vary.

Chapter 3 - An inquiry into the use of indoor CO_2 and humidity ratio trend data with inverse modelling to estimate air infiltration

This chapter has been submitted for publication as:

An inquiry into the use of indoor CO_2 and humidity ratio trend data with inverse modelling to estimate air infiltration

Z. Xiong; J. Berquist; H. B. Gunay; C.A.Cruickshank, *Building and Environment*

3.1 Introduction

Air infiltration is one of the most influential parameters for building energy performance and indoor environmental quality. Previous research [34–40] reports that air infiltration is the third most influential factor of energy consumption, accounting for 15% to 50% of annual heating and cooling energy consumption in commercial buildings in the United States. In addition to the energy concerns associated with building infiltration, it may transport undesired airborne pollutants, such as fungal spores, radon, air bio-contaminants, and particulate matter [38, 39, 41–44] , which may have adverse health impacts on occupants. High infiltration rates can also trigger thermal discomfort and low indoor relative humidity (RH) in cold climates [32]. Furthermore, the occurrence of concealed condensation in the building envelope components increases due to moisture accumulation caused by air infiltration, which can detrimentally affect the properties of the building envelope [45–47]. Thus, building airtightness must be taken into account to ensure high building performance.

A substantial research effort has been devoted to infiltration in residential buildings over the past 30 years [34, 35, 46–48]. During this period, two field-scale airtightness tests have become very common in residential buildings: fan pressurization and tracer gas tests. The airtightness characteristics of single-zone buildings are often determined through a standard fan pressurization

test in accordance with CGSB 149.10 – M86 and ASTM E779 [11, 49]. This method aims to measure the air leakage rate at standardized air pressure differences and fit these data to a power-law curve. Micromanometers are used to monitor pressure differences which need to be converted to volumetric airflow rates under pressurized or depressurized conditions [11]. Blowers or fans are used to pressurize or depressurize a single enclosed zone until the pressure difference between the indoor and outdoor ranges from 50 Pa and 75 Pa; however, they do not ensure uniform-pressure conditions throughout the space. As a result, this method is generally less compatible with commercial buildings because it necessitates additional fans to provide uniform pressurization in the entire building, turning into a labour-intensive and costly experimental setup. The fan pressurization method also needs trained staff for operation, and the noise generated by installing, unloading, and operating equipment may disturb building occupants. Other potential shortcomings, such as the human errors caused by operators, the uncertainties derived from meteorological data and internal/external pressure, the non-uniformity of building pressure, and obstacles in pinpointing envelope imperfections, may degrade testing accuracy and make fan pressurization tests less suitable for commercial buildings than small residential sectors [39, 40, 50].

In addition to fan pressurization tests, tracer gas testing can be used to measure air infiltration rates. According to the ASTM E741 [9], tracer gas testing is more beneficial for directly measuring the air change rate at natural pressure differences in commercial buildings. Tracer gas tests determine the air change rate of an enclosed zone by releasing a tracer gas and measuring its concentration. Three typical testing methods are usually applied: the concentration decay method, the constant injection method, and the constant concentration method [49].

For the concentration decay method, the tracer gas is dosed within an enclosed zone until reaching an expected value. Then, measuring the concentration of the decay period after mixing the air uniformly through a mixing fan. The constant injection method requires introducing tracer gas at a constant flow rate until the concentration reaches an equilibrium. The constant concentration method is usually considered the reference method [49]. It uses an automated injection device to help maintain a target tracer gas concentration. Cui et al. [18] summarized four main boundary conditions that restrain the utility of tracer gas. The ideal tracer gas should be risk-free for occupants and properties, insensitive to surroundings, quantifiable by instruments, and easily recognized from mixing air. Specifically, the tracer gas should be harmless and non-burnable to ensure occupants' safety and building properties and be insensitive to the environments to ensure accurate measurements of the indoor concentration of tracer gas. Meanwhile, the tracer gas should be readily recognized from the air mixture and measured by sensors or gas analyzers. Most of the currently used tracer gases have limitations. For example, isotope radioactive tracer gases, e.g., ^{86}Kr, are costly and not readily available. Another common tracer gas, sulphur hexafluoride (SF_6), is a potent greenhouse gas that is non-toxic but has a global warming potential (GWP) of 22800 over 100 years; which has caused its use as a tracer gas to be banned by the European Union.

Although tests with these conventional tracer gases have been carried out many times in the industry, they still suffer some drawbacks. Compared to traditional tracer gases, such as SF_6, perfluorocarbon tracers (PFTs), carbon monoxide (CO), and nitrous oxide, CO_2 is a potential alternative that can be implemented on multi-zone commercial buildings. CO_2 is non-explosive and non-toxic (at low concentration) and exists at a relatively constant ambient concentration, at least at the timescale of these experiments [18]. Although CO_2 as a tracer gas has advantages, the

conventional tracer gas test needs a large amount of CO_2 to be injected into target zones that may disturb buildings' daily use. Thus, a few researchers [52–54] proposed using the occupant-generated CO_2 as a tracer gas instead of injecting the CO_2 into the target zone to investigate the airtightness of commercial buildings. Meanwhile, CO_2 sensors can help measure CO_2 concentration since they have become easily accessible in recent years due to the widespread use of demand-controlled ventilation in building automation systems (BASs).

Turiel and Rudy [50] reported that the CO_2 concentration generated by occupants could be treated as an indicator of airtightness. They conducted different tracer gas tests using SF_6 and occupant-generated CO_2 as a tracer gas and found that the infiltration rates obtained from the two tracer gases had good agreement with each other. Batterman [51] provided a review of the occupant-generated CO_2 method with four testing techniques, including the transient mass balance method, steady-state method, build-up method and concentration decay method. They monitored the air change rates of four classrooms during unoccupied hours using the CO_2 decay method, which provided reasonable results. Similar to Turiel and Rudy [50], Claude-Alain and Foradini [52] used the occupant-generated CO_2 decay method to investigate the air change rate of a private room in a building experimentally and validated it with an SF_6 tracer gas test. They corroborated that this approach is feasible and may become a possible surrogate of conventional methods.

Water vapour, generated by occupant activities, is another opportunistic tracer gas. Giesbrecht et al. [13] conducted humidity ratio-based decay experiments in three buildings to investigate whether the water vapour was capable of measuring ventilation rates. The first building was an indoor swimming pool with waterproof walls, ceilings, and floors. The second building was a conventional house with normal furnishings (e.g., extensive carpets, latex-painted gypsum board walls, and ceilings), while the third building was also a house but furnished with thick

carpets and unpainted gypsum boards. Nitrous oxide (N_2O) was used to validate the results calculated from the humidity ratio-based decay method. The results showed that the humidity ratio-based decay method was in the best agreement with the N_2O testing results in the indoor swimming pool ($\pm$ 0.04 h^{-1}). By contrast, this method was not reliable in conventional houses furnished or constructed with hygroscopic materials.

Both conventional tracer gas tests and occupant-generated CO_2 tracer gas tests are sensitive to experimental conditions. They can track the instantaneous infiltration rates of a zone. However, tracer gas tests require experimental apparatus such as devices for tracer gas injection, concentration monitoring and data acquisition; they are labour-intensive as trained technicians are required to carry out the experiments; they can be disruptive for the building operations as the odour of tracer gases and the noise of experiment operation are able to annoy occupants, as well as turning off the HVAC system to ensure the accuracy of test measurements. Thus, they are more appropriate to small residential sectors rather than large commercial buildings.

3.1.1 Background and previous work

To address the limitations of conventional airtightness tests mentioned above, an inverse model-based method was proposed. According to the ASHRAE Handbook – Fundamentals [53], two common inverse model formalisms exist; the black-box approach and the grey-box approach. Examples of the black-box approach are machine learning and regression models, which can be built based on statistical principles or engineering formulation. In contrast to the black-box approach, the grey-box approach relies on simple physical models and requires high-level user expertise. Typically, inverse models are used to characterize and monitor the performance of existing systems and their properties. They are often driven by different sets of variables and

empirical parameters in different conditions [55]. Although inverse modelling has been developed in various fields for several decades, only a few studies have employed it to investigate infiltration rates. The remainder of Section 1.1 introduces previous inverse model-based approaches for infiltration estimation using various techniques.

Ng and Wen [54] developed a grey-box building airflow network model to determine the airflow rates, the inter-zonal airflow rates and the ventilation system return airflow rates based on CO_2 concentration. Three parameter estimation techniques were proposed to solve the airflow network: least-squares, nonlinear parameter optimization, and nonlinear parameter optimization with a stochastic term method. In Ng and Wen's study, the airflow rates estimated by simulated CO_2 concentration were compared with the simulated airflow rates. The results showed that the least-squares method performed well. Meanwhile, the estimated airflow rates were in good agreement with the simulated values with a mean error of less than 0.5 h^{-1}.

Hong and Lee [55] proposed an inverse modelling approach to estimate zone infiltration rates and zone thermal mass. The simulated zone air temperature data generated from the U.S. Department of Energy (DOE) reference building [56] was used to train the inverse model. The results exhibited that this novel approach intensified the accuracy of energy simulation. To investigate air infiltration rates, Li et al. [57] developed an inverse model as well. The simulated measurements, including zone air temperature, humidity ratio, and CO_2 concentration, were implemented in the inverse model. The infiltration rates were estimated under three different HVAC system operating scenarios. The most accurate infiltration estimates were gained from CO_2 concentration and humidity ratio when the HVAC system is on, and the HVAC system details are known within all measurable parameters. The authors also concluded that the CO_2 concentration

is less affected than the humidity ratio by environmental factors; thus, CO_2 concentration was found in the best agreement with the ground truth of infiltration rates.

Xiong et al. [58] established an inverse model based on the CO_2 concentration decay at unoccupied hours. The CO_2 generated by occupants measured by the air handling unit (AHU) return air CO_2 sensors in three commercial buildings were used to investigate the air infiltration rates in lieu of simulated data. The results showed that inverse models could help monitor the variation of building airtightness over the years using existing return air CO_2 sensors; however, an advanced model is required to filter out more accurate infiltration estimates.

Gunay et al. [59] also developed various inverse models to estimate building thermal transmittance and infiltration in two office buildings. The outdoor temperature and horizontal solar radiation, indoor temperature and CO_2, and heating data extracted from BASs were used to train models. The authors reported that inverse modelling could be treated as a diagnostic tool to track airtightness over time.

Published studies demonstrated that inverse modelling shows promise for investigating air infiltration rates. To the best of our knowledge, this approach is rarely used and lacks case studies and field experiments. The existing inverse models were trained using simulated measurements rather than field-scale data, which may not correctly reflect the uncertainties in infiltration rates under real-world conditions. Thus, this research aims to substantiate the applicability and the potential of the inverse model-based method in estimating air infiltration rates.

3.1.2 Motivation and objectives

Due to the widespread use of BASs and smart thermostats in recent years, CO_2 and RH measurements are becoming increasingly available. Aside from monitoring indoor air quality and occupant-centric ventilation, CO_2 and RH sensors in BAS thermostats (hereafter will be

abbreviated as BAS-grade sensors) and sensor hubs can provide opportunities to estimate air infiltration rates. This provides the potentiality of the use of low-cost CO_2 and RH sensors in thermostats and sensor hubs. Inverse models can be employed to filter out infiltration rates from natural fluctuations in the CO_2 concentration and humidity ratio subject to day-to-day variations in the occupancy and occupant activities. This will enable monitoring airtightness continuously and provide a benchmark to track infiltration characteristics as an operational tool – thus, changes in airtightness over time can be constantly monitored and anomalies can be detected. Even though the inverse model-based approach is also applicable to a single-family residential building, the lack of BASs in residential buildings limits its employment. Thus, this method is more appropriate for commercial buildings due to the availability of BAS trend data and the particular challenges associated with conducting airtightness tests in large commercial buildings. To this end, the inverse model-based approach to calculate infiltration rates is investigated with indoor CO_2 and humidity ratio data extracted from commercial buildings.

The objective of this chapter is to develop a low-cost and practical inverse model-based approach to continuously estimate the air infiltration rate by using existing CO_2 and RH sensors. The case study and experimental results presented in this chapter were used to answer three research questions: 3-1) Can the BAS-grade CO_2 sensors be used to estimate air infiltration rates instead of standalone CO_2 data loggers? 3-2) Can humidity ratio (r_w) be treated as a tracer gas for estimating infiltration? And 3-3) can an inverse model filter out the infiltration rates from BAS trend data for CO_2 and humidity ratio?

3.2 Methodology

The methodology follows three parts: formulate the mathematical models, preprocess the data, and describe the case study. The mathematical models detailed in Sections 3.2.1 and 3.2.2 are based on the conventional tracer gas concentration decay method. Section 3.2.3 describes the necessary steps that need to be considered before employing the model. Section 3.2.4 provides information on the case study, including a brief overview of test spaces, the procedures of conducting tracer gas tests, and the instrumentation used in this study.

3.2.1 CO_2-based linear regression

Assuming a single well-mixed zone located in a recently vacated building after the mechanical ventilation system is turned off, the following differential equation defines the CO_2 decay behaviour:

$$\frac{dC}{dt} = (C_t - C_{oa}) \cdot \frac{q_{inf}}{V} \quad (3.1)$$

where C_t is indoor CO_2 concentration at time *t*, q_{inf} is the average air infiltration rate in m^3/s, and *V* is the volume of the single zone in m^3. The bias in each CO_2 sensor is reflected in the C_{oa} value. For example, if the lowest indoor air CO_2 concentration for a specific sensor was recorded to be 380 ppm over a long period, then the C_{oa} is set to be 380 ppm.

Subsequently, Eqn. 3.1 is discretized using a first-order forward difference approximation:

$$C_{t+\Delta t} - C_t = (C_t - C_{oa}) \cdot \left(\frac{q_{inf}}{V} \cdot \Delta t\right) \quad (3.2)$$

where the difference between C_{t} and $C_{\mathrm{t+\Delta}t}$ represents the variation of CO_2 concentration over the timestep Δt. Note that multiplying the term $\frac{q_{inf}}{V}$ with 3600 seconds will provide the normalized

infiltration metric air changes per hour (h^{-1}). Note that $q_{\inf}$ is the average infiltration rate, and it is the unknown parameter of this regression problem.

3.2.2 Humidity ratio-based linear regression

According to ASHRAE Fundamentals [53], the humidity ratio is calculated based on atmospheric pressure (P_t), the saturated vapour pressure (P_{sw}), and vapour pressure (P_w) in P_a:

$$P_{sw} = e^{\left(16.65-\frac{4030.183}{T+235}\right)} \times 1000 \quad (3.3)$$

$$P_w = RH \times P_{sw} \quad (3.4)$$

$$r_w = \frac{P_w}{P_t - P_w} \times 0.622 \quad (3.5)$$

where T is the temperature in ℃, RH (%) is relative humidity measured by sensors, P_t is atmospheric pressure about 101,300 P_a at sea level, and r_w is the humidity ratio, which represents the water vapour content per 1 kg of dry air.

Similar to the CO_2-based regression model shown above, the time-varying humidity ratio is used to characterize the moisture decay trend of indoor air after the AHU is shut down:

$$r_{w,t+\Delta t} - r_{w,t} = (r_{w,t} - r_{w,oa}) \cdot \left(\frac{q_{inf}}{V} \cdot \Delta t\right) \quad (3.6)$$

3.2.3 Dara preprocessing

Two datasets, the tracer gas testing data and historical data, were used to estimate the unknown parameter q_{inf} in equations (3.2) and (3.6). The tracer gas tests with CO_2 and humidity ratio were conducted to answer the research question (3-1) regarding the usability of BAS-grade CO_2 sensors instead of standalone CO_2 loggers and research question (3-2) regarding the usability of humidity ratio as a tracer gas. Procedures followed in these tracer gas tests are detailed in the following subsection.

The historical BAS trend data were extracted from the rooms in which the tracer gas tests were conducted to answer the research question (3-3) regarding the proposed method's ability to filter out q_{inf} from naturally occurring daily CO_2 and humidity ratio patterns.

The following preprocessing steps were applied to the historical trend data:

1. Include periods when AHU fans and humidifier were off;
2. Include periods when indoor CO_2 concentration/humidity ratio was well above the outdoor CO_2 concentration/humidity ratio;
3. For CO_2 sensors, remove the sensor bias by shifting the measurements by the difference between the minimum recorded sensor reading and the expected outdoor CO_2 concentration (400 ppm).

Note that the filtering criteria explained above aim to isolate unoccupied hours while occupants' impact on indoor CO_2 and humidity levels still exists. Filtering out periods when the mechanical ventilation systems are operational were required to eliminate the effects of these systems on the building's pressurization, in turn, on the infiltration process.

3.2.4 Case study

The tracer gas tests were conducted in three adjacent identical offices with fixed windows located in a 6,500 m^2 academic office building in Ottawa, Canada. Figure 3.1 presents the devices used in the experiment, including three CO_2 releasing kits, (i.e., a 5 lb aluminum CO_2 cylinder, a regulator, a gas tube, and a seal per kit), three humidifiers with fans, three new standalone data loggers (with recent calibration certificates), and three commercial thermostats with built-in CO_2 and RH sensors integrated with the BAS. These two measuring tools were selected to simultaneously measure the indoor CO_2 and RH variations during the experiment; thus, the infiltration rates were estimated by the BAS data, and the data loggers could be compared to

determine whether this method is applicable in using BAS-grade sensors (research question 3-1). The fan on the top of the evaporative humidifier is responsible for fanning out the humidified air and mixing the tracer gas with the indoor air.

Table 3.1 tabulates the characteristics of the data logger and BAS sensor. These two measuring tools were selected to measure the indoor CO_2 variation simultaneously during the experiment, thus, the average infiltration rates estimated by the BAS data and the logging data can be compared to determine whether this method is applicable in using normal CO_2 sensors. Note that the BAS-grade sensors have been installed on the wall and have not been calibrated for several years.

Table 3.1: The specifications of data logger and BAS sensors

Type	Data Logger (CO_2 sensor) [60]	Data Logger (RH sensor) [60]	BAS-grade CO_2 sensor [61]	BAS-grade RH sensor [61]
Measurement Range	0 – 5000 ppm	1% - 90%	0 – 2000 ppm	1% - 90%
Accuracy	±50 ppm + 5%	± 2%	±50 ppm + 2%	± 3%
Response Time	1 min	1 min	-	-
Sensing Method	Non-dispersive infrared (NDIR) absorption	-	Non-dispersive infrared (NDIR) absorption	-
Manufacture	Onset HOBO MX1102A	Onset HOBO MX1102A	Delta DNS-24	Delta DNS-24

Figure 3.1: Experimental devices (from left to right): (a) CO_2 releasing kit, (b) data logger, (c) thermostat with built-in BAS sensor, and (d) the evaporative humidifier.

Figure 3.2 presents the layout of the offices and the approximate locations of these devices. The data logger is placed on top of a bookshelf in each office, where it is closest to the pre-installed thermostat and is 1.5 meters above the floor.

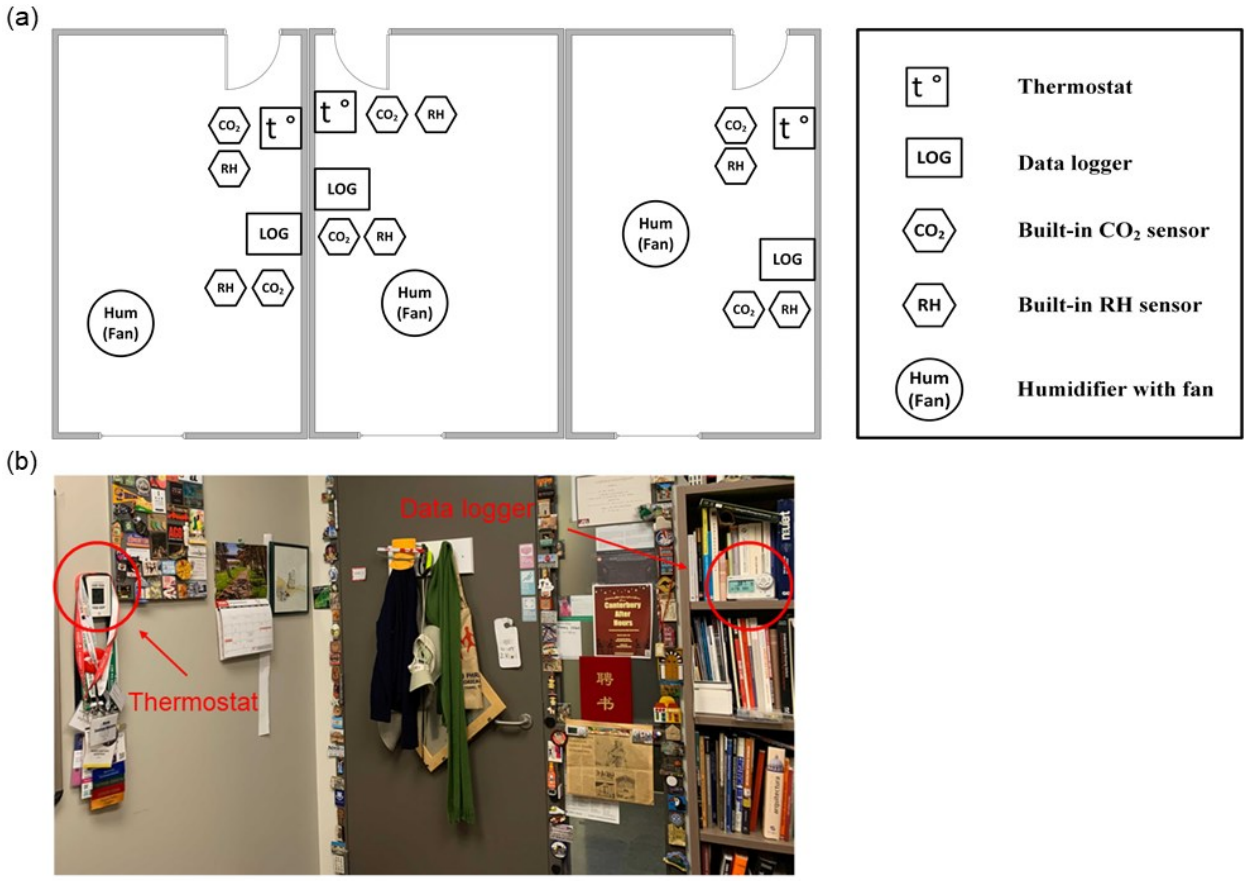

Figure 3.2: (a) The schematic of Office 1 (left), Office 2 (middle), and Office 3 (right). (b) Photo of the middle office.

Before experiments were started, all target zones were manually checked to be unoccupied, with doors closed. Also, the indoor and outdoor temperature, wind speed, and wind direction were recorded. At the beginning of the experiment, the humidifiers were turned on to increase indoor RH levels. Then CO_2 was dosed into the confined area through the releasing kit until the indoor CO_2 concentration exceeded 1500 ppm. Some key elements need to be emphasized during the experiment. First, the CO_2 was released at different positions, and the fans were operational to ensure the uniformity of the indoor mixture during the dosing period. Second, experimenters left

target zones after they stopped humidifying and releasing CO_2, and the data logger and BAS-grade sensor were set to record the RH and CO_2 concentration at the moment of release, mixing and decay of RH and CO_2 concentrations. Note that RH measurements were not directly used for infiltration estimation but for calculating humidity ratio, as mentioned in the previous subsection. Two additional factors need to be considered before starting the analysis. First of those is the appropriate interval for choosing tracer gas testing data. The aim was to select the data which can best represent the stable decay of the indoor air mixture under the condition that the indoor air mixed uniformly. The second factor influencing the tracer gas test was the air exchange between adjacent offices during the measuring period. To this end, experiments were conducted in three offices simultaneously during the first two experimental days (Day 1 and Day 2) to investigate the zonal infiltration rates. In contrast, only the middle office (Office 2) was chosen to artificially increase CO_2 concentration and humidity level in the following two days (Day 3 and Day 4) for the observation of inter-zonal airflow. Note that data only collected from Office 2 on Day 1 and Day 2 were used to estimate the infiltration rates. The aim of conducting tracer gas tests in adjacent offices was to create similar environmental conditions so the inter-zonal air exchange can be assessed and minimized.

Table 3.2 summarizes the characteristics of the data used. The tracer gas tests were repeated twice to quantify repeatability on two consecutive evenings. Thus, two 30-minute interval datasets collected from standalone data loggers and BAS-grade sensors were used to train the regression models separately. The infiltration rate estimates from the data loggers and BAS-grade sensors were compared for both CO_2 and humidity data with the repeated experiments.

Furthermore, historical indoor CO_2, temperature, and RH data of five workdays in the same office were extracted from the BAS based on the aforementioned filtering criteria. These data were used

to check the applicability of inverse modelling under normal conditions (i.e., using the occupant-generated CO_2 and humidity) rather than tracer gas tests (research question 3-3).

Table 3.2: The characteristics of tracer gas testing data and historical data selected from three private offices (Note "-" indicates that the data provided by the data logger was not available).

Data	Data Type	Data Interval	Number of CO_2 Sensors	Number of RH Sensors	Number of Data Loggers
Tracer Gas Testing Data	Numeric	30 minutes	1 per office	1 per office	1 per office
Historical Data	Numeric	1 hour	1 per office	1 per office	-

3.3 Results and Discussion

This section presents the data preprocessing and the average infiltration rates of Office 2 that were estimated using tracer gas testing data by treating both CO_2 and humidity ratios as the tracer. The results estimated by historical data are presented as well. Finally, potential factors that may influence the modelling results and the prerequisites of applying the proposed approach are discussed.

3.3.1 Data preprocessing

An important decision in tracer gas testing is to select the interval of experimental data to estimate infiltration rates. Both are using data before the completion of the mixing process, and discarding valuable experimental data detrimentally affect the accuracy of the infiltration estimates. To this end, a sensitivity analysis was conducted by varying the intervals of data used in estimating the infiltration rates.

Figure 3.3 shows the variability of R^2 values of inverse models that were estimated from different intervals. The proposed inverse model-based approach was used to calculate infiltration rates and R^2 at various intervals of tracer gas testing data, and the interval which produced the highest R^2 would be selected for the following analysis. Results estimated from both the BAS-

grade sensor and standalone data logger of Office 2 on two experimental days were calculated for comparison. Note that the humidifier was turned on at 7:00 pm and turned off at 8:00 pm, while CO_2 was dosed at 8:00 pm and stopped within 3 minutes. Thus, the data measured after 9:00 pm were selected to ensure the indoor CO_2 and humidity were uniformly distributed. Meanwhile, since the AHU was entirely open at 7:00 am, the data collected after 6:30 am were discarded to eliminate the influence of the mechanical ventilation system.

According to trends of variation, what stands out in Figures 3.3 (a) and 3.3 (b) is that R^2 values calculated by CO_2-based tracer gas tests for all intervals are 0.99. Each dot represents the R^2 value obtained from data with different experimental intervals. For example, the dot annotated at 3 am represents the R^2 value calculated by data collected from 9:00 pm to 3:00 am, while the dot annotated at 3:30 am represents it using the data from longer hours. This indicates that any measurement period of CO_2-based tracer gas tests is appropriately used to estimate infiltration rates. However, the concentration of tracer gas should not be too close to the outdoor level. Therefore, the CO_2 data collected from 9:00 pm to 5:30 am were applied to the inverse model. Similar to CO_2-based tracer gas tests, Figure 3.3 (c) and 3.3 (d) exhibit the R^2 values obtained using humidity ratio trend data. The interval chosen for the humidity ratio-based analysis was from 9:00 pm to 3:00 am, since the highest R^2 appeared when using a stop time of 3:00 am on Day 1 and Day 2 for both BAS-grade sensor and standalone data logger.

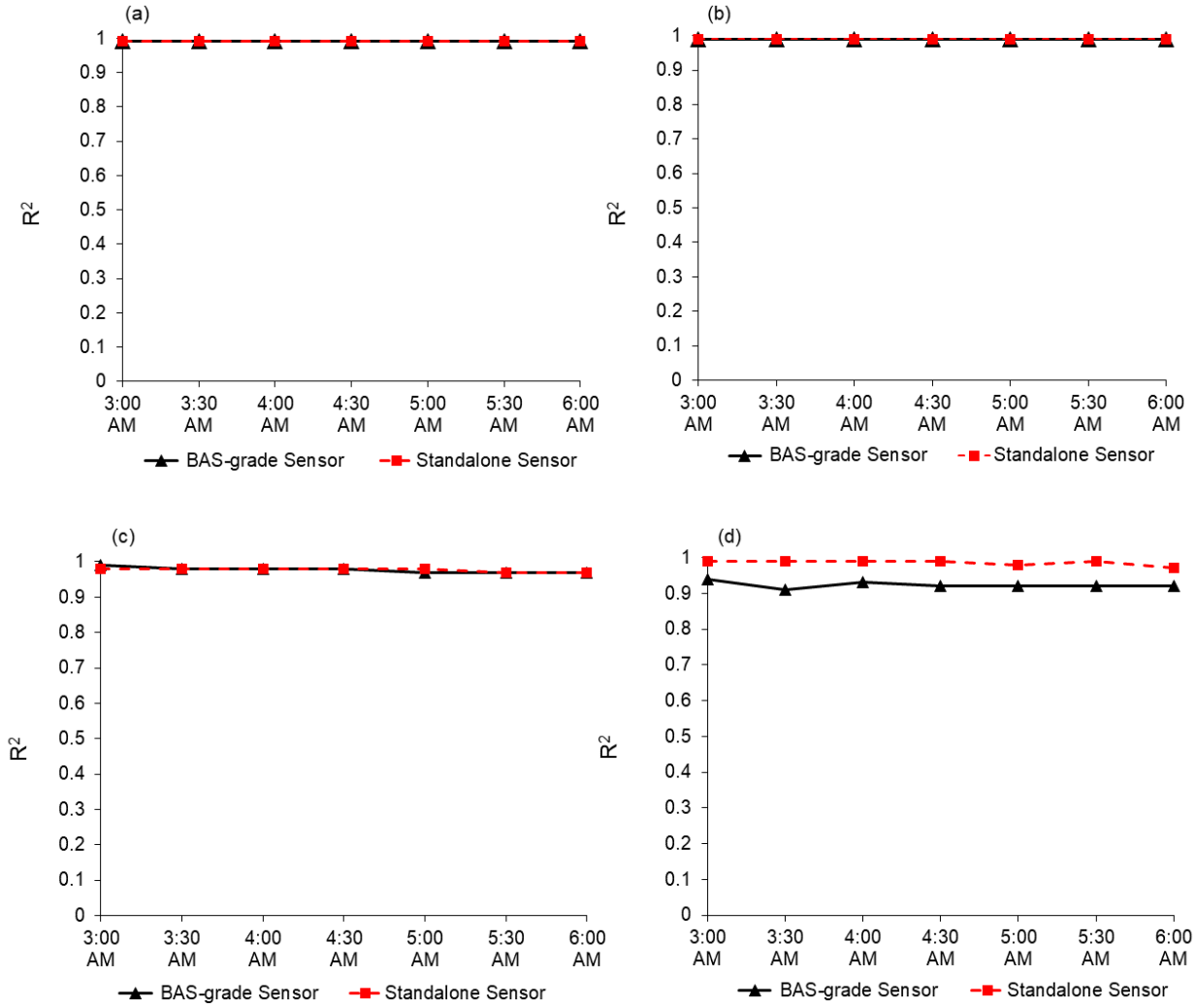

Figure 3.3: The variation of R^2 values of different inverse models for different time intervals in Office 2. The CO_2-based tracer gas tests were conducted on (a) Day 1 and (b) Day 2, and the humidity ratio-based tracer gas tests were conducted on (c) Day 1 and (d) Day 2 instantaneously. The "BAS-grade Sensor" represents the R^2 values of inverse models calculated by data collected through the BAS-grade sensors; the "Standalone Sensor" represents the R^2 values of inverse models estimated by data collected.

Inter-zonal airflow was another concern that needed to be considered before beginning the tracer gas testing analysis and historical analysis. The internal temperature and pressure difference between zones would result in the indoor airflow passing through adjacent rooms, which will influence the accuracy of measurements, in turn, the estimated infiltration rate. Therefore, conducting tracer gas tests only in Office 2 was used to assess whether the inter-zonal airflow should be included in the present study.

Figure 3.4 shows the concentration decay of CO_2 concentration and humidity ratio for Office 2. Both CO_2 concentration and humidity ratio increase sharply and decay rapidly in Office 2. The shaded area represents the data collecting interval mentioned above. As shown in Figure 3.4 (a), the CO_2 concentration in Office 1 and Office 3 slightly fluctuates when the CO_2 in Office 2 varies significantly. Unlike the simultaneous variation of CO_2 concentration, the humidity ratio of the adjacent offices (Figure 3.4 (b)) gradually and slowly increases when the one in Office 2 increases significantly, whereas they continue to rise when the middle-office values decay and converge at 3:00 am. The humidity ratio of Office 1 and 3 peaks the next morning and suddenly decreases at 7:00 am after the AHU is turned on. The possible explanation of these delayed increases of humidity ratio is delayed responses of RH sensors in adjacent rooms. Since the objectives of this study are to verify whether BAS-grade sensors can replace standalone sensors in tracer gas tests (research question 3-1) and whether the humidity ratio is a potential tracer gas (research question 3-2), the delayed responses of RH sensors do not affect the conclusion of this study. As Office 1 and Office 2 had minimal changes in indoor CO_2 concentration and humidity ratio that can be negligible (the shaded parts), the inter-zonal airflow is excluded in this study. However, the air exchange between the hallway and test office was still included as the door gap was not sealed during data collection.

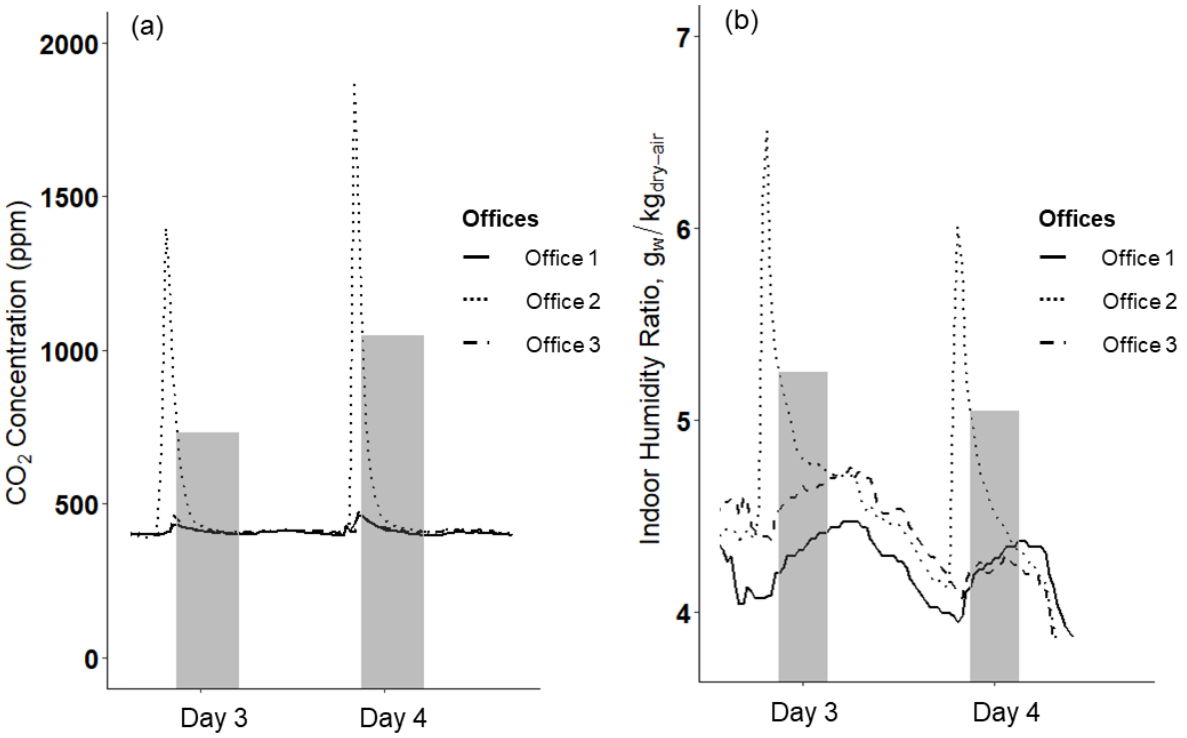

Figure 3.4: The time-varying (a) indoor CO_2 concentration and (b) humidity ratio in three private offices on the third and fourth experiment day. The shaded area represents the intervals (10 pm to 5:30 am for CO_2, 9 pm to 3 am for humidity ratio) selected to train the regression model. Office 2 (the middle office) was injected with CO_2 and humidity; data for the rooms adjacent to Office 2 were plotted to inspect inter-zonal air leakage.

3.3.2 Tracer gas testing data

The tracer gas tests were conducted twice in two days for repeatability. The following time-series plot (Figure 3.5) shows the variation of indoor CO_2 concentration in Office 2. The initial indoor CO_2 concentration of the unoccupied office was around 400 ppm on both days, and it increased rapidly after starting to dose CO_2 at 8:00 pm. Then the downward trend appeared after stopping the release and lasted until the following day. The shaded areas represent the ranges of selected data that are from 9:00 pm to 5:30 am. We define the time ranges from 9:00 pm to midnight as "late night" while the time ranges from midnight to 5:30 am as "early morning" of the following day. Figure 3.6 presents the exponential decay curves of indoor CO_2 concentration for

different infiltration rates. The red curve represents measured CO_2 variation in the tracer gas test, while the rest were added as visual references for interpretation.

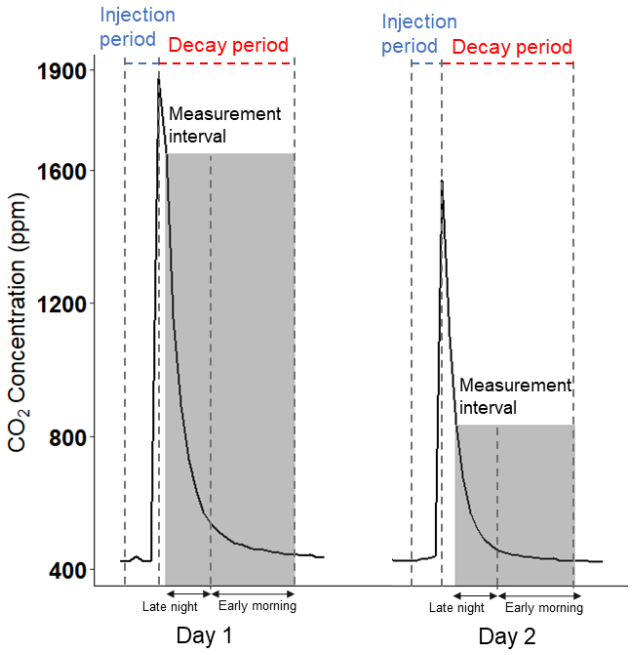

Figure 3.5: The fluctuation of indoor CO_2 concentration is divided into an injection period and a decay period. The data used in the linear regression model were only selected from the late night and early morning.

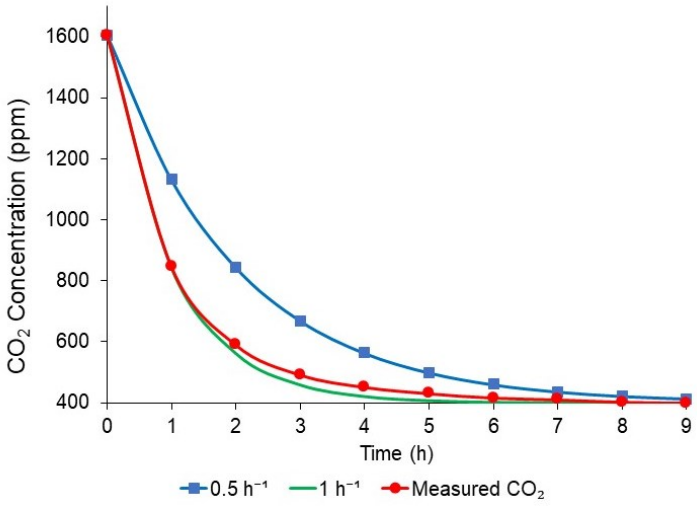

Figure 3.6: Exponential decay curves of CO_2 concentration in Office 2 on Day 1

The average infiltration rates of Office 2 are tabulated in Table 3.3. The results obtained in two days were in the range of 0.77 h^{-1} to 0.83 h^{-1}. The highest (0.83 h^{-1}) and lowest (0.77 h^{-1}) average infiltration rates were estimated from the data collected on Day 1 and Day 2, respectively. By comparing the results recorded from different devices in the same office on the same day, the most considerable inter-sensor variation is 0.05 h^{-1} on Day 1, whereas the lowest inter-sensor variation is 0.03 h^{-1} on Day 2. All results listed in Table 3.3 have p-values calculated from the inverse model approach (Eqn. 3.2) less than the significance level (0.05) and R^2 values at 0.99, indicating that the proposed inverse model fits CO_2-based tracer gas testing data well and is reliable to explain 99% variation of the data. From all cases of different results, it can be observed that BAS-grade sensors and data loggers are generally consistent on both days, indicating that BAS-grade sensors were capable of estimating the infiltration rates (research question 3-1).

Table 3.3: Comparison of experimental results based on the CO_2 data collected by the data logger and BAS-grade sensor.

Day 1		Day 2	
Data Logger (h^{-1})	BAS-grade Sensor (h^{-1})	Data Logger (h^{-1})	BAS-grade Sensor (h^{-1})
0.83	0.78	0.80	0.77

Figure 3.7 shows the variation of indoor humidity ratio during the first two days of experiments, which were calculated by the RH and indoor temperature data. The indoor humidity increased to 6.7 $g_w/kg_{dry\text{-}air}$ after the humidifier was turned on for one hour. After the humidification of indoor air was stopped, the humidity ratio began to decrease over time. Same as the fluctuation of CO_2 concentration shown above, the humidity ratios in the shaded areas were used to train the proposed model and calculate the infiltration rates. The "late night" for humidity ratio-based tracer gas tests was defined from 9:00 pm to midnight, while the "early morning" was defined from 12:00 am to 3:00 am. Analogous to Figure 3.6, Figure 3.8 illustrates exponential decay curves for different infiltration rates based on humidity ratio.

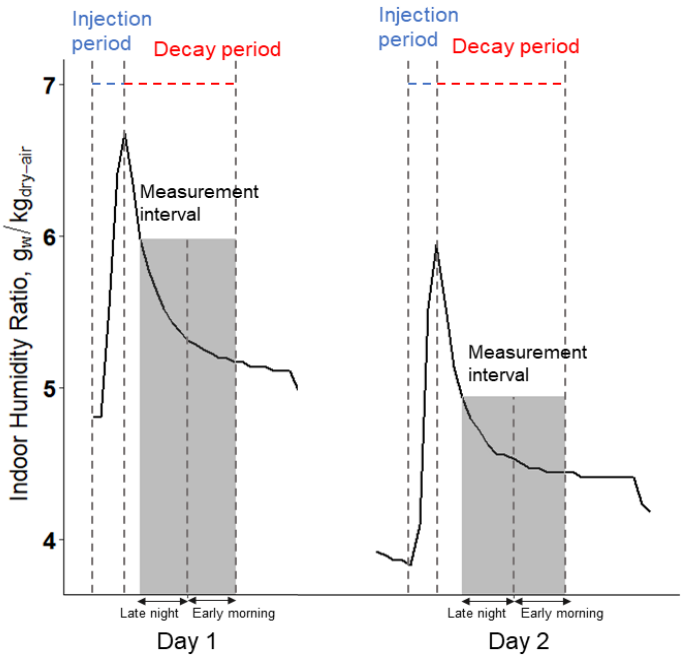

Figure 3.7: The variation of indoor humidity ratio during the two experiment days in Office 2.

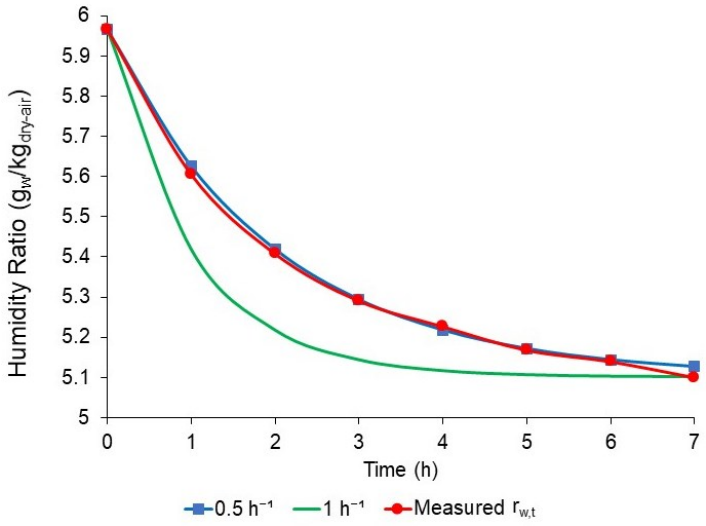

Figure 3.8: Exponential decay of indoor humidity ratio in Office 2 on Day 1.

Table 3.4 lists the average infiltration rates estimated by humidity ratio data. The range of results is 0.49 h^{-1} to 0.54 h^{-1}. The most considerable inter-sensor difference on Day 1 in Office 2

is 0.03 h^{-1}, whereas the smallest difference is 0.01 h^{-1} on Day 2. The possible explanation is relative to adsorptive and desorptive effects that are provided in Section 3.4 with details. The p-value estimates of all results on two days are zero, and R^2 values of each day are 0.98 and 0.99 for standalone data loggers and 0.99 and 0.94 for BAS-grade sensors. This scenario indicates that the inverse model is statistically significant and reliable when applying humidity ratio data (research question 3-2). There are comparatively apparent differences between the infiltration rates estimated by humidity ratio (Table 3.4) and those obtained from CO_2 concentration (Table 3.3) on the same day. The most noticeable difference was on Day 1, which is 0.29 h^{-1} for the standalone data logger (0.83 h^{-1} with CO_2 vs. 0.54 h^{-1} with humidity ratio).

Table 3.4: Comparison of tracer gas test results based on the humidity ratio data.

Day 1		Day 2	
Data Logger (h^{-1})	BAS-grade Sensor (h^{-1})	Data Logger (h^{-1})	BAS-grade Sensor (h^{-1})
0.54	0.51	0.49	0.50

It is worth noting that weather conditions needed to be considered for both CO_2-based and humidity ratio-based tracer gas tests. Although there were only slight differences in wind speed, wind direction, and outdoor temperature between Day 1 and Day 2, the day-to-day variation can be partly attributed to these differences. According to the meteorological data obtained from Ottawa International Airport, there was a temperature difference of 3 ° C between two days, and the wind blew from north-west to south-east on Day 1 at 13 km/h, while the wind blew from south to north on Day 2 at 5 km/h. Note that the academic building is located north of the airport. Thus, the time-varying fluctuation of outdoor airflow may affect day-to-day experimental results. It should also be noted that it rained on Day 1, resulting in slightly higher outdoor humidity ratio levels.

The measurement errors are mainly responsible for explaining the inter-sensor difference in infiltration rates estimated on the same day. Firstly, we cannot prove the indoor air is perfectly mixed one hour after releasing CO_2, although we have used a fan to promote air mixing. Different manufacturers of measuring devices are another possible factor that influences the CO_2 measurements, in turn, infiltration estimates. Calibration is also regarded as one of the factors affecting the accuracy since the BAS-grade sensors have not been calibrated for more than five years, whereas the data loggers were calibrated before the experiments. Besides, Buggenhout et al. [62] indicated that the sampling positions contribute to the measurement errors in the tracer gas concentration decay method as well. As mentioned earlier, although the standalone data logger was placed as close to the BAS-grade sensor as possible, there was still a height difference between them. As a result, the testing data measured by them were not exactly the same, which may also increase the uncertainty of the results.

3.3.3 Historical data

Aside from the tracer gas test analysis, occupant-generated CO_2 and humidity data of Office 2 were obtained from the BAS. The data were extracted from five workdays in Office 2 in winter based on the filtering criteria mentioned above (i.e., unoccupied hours, AHU was shut down), and the average infiltration estimates were reported in this section. The historical data were processed to assess our ability to estimate infiltration rates from the natural day-to-day variations of the indoor humidity ratio and CO_2 levels without dosing a tracer gas (research question 3-3).

The linear correlation of two variables based on equation 2 has been presented in Figure 3.9. After applying the aforementioned filtering criteria, the scatter plot illustrates a strong, positive, linear relationship between the time-varying indoor CO_2 concentration (y-axis) and the difference between indoor and outdoor CO_2 concentration (x-axis). The linear equation shown in Figure 3.9

is estimated following equation 2, and the slope of the trend line represents the predicted average infiltration rate in h^{-1} of Office 2, which was 0.7 h^{-1}.

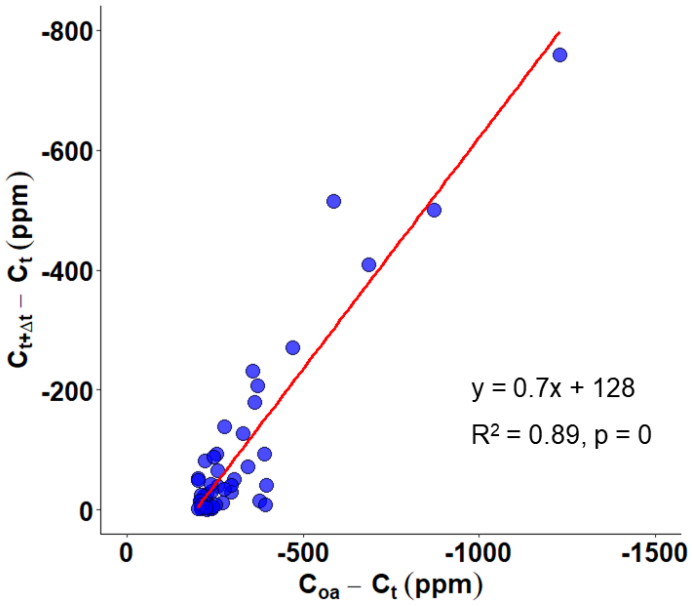

Figure 3.9: The coefficient of a trend line created between the indoor CO_2 concentration interval and the CO_2 concentration difference between indoor and outdoor represent the average infiltration rate for Office 2. The CO_2 concentration data used to create the linear regression model were collected by a BAS-grade sensor.

Table 3.5 presents a summary of the estimated average infiltration rate of Office 2 and its statistical significance. Since the p-value was less than 0.05, the slope was interpreted as statistically significant. Specifically, the variations in indoor-outdoor CO_2 concentration ($C_{oa} - C_t$) correlates strongly to the rate of change in the indoor CO_2 concentration ($C_{t+\Delta t} - C_t$). The R^2 was 0.9, indicating that the proposed inverse model can explain 90% of the variation within historical CO_2 data. Recall that the target office's infiltration rates estimated from tracer gas tests range from 0.77 to 0.83 h^{-1}. The estimate of inverse modelling with historical CO_2 data (0.7 h^{-1}) for the same office is close to tracer gas testing results; thus, the proposed inverse model-based approach appears to be a practical alternative to filter the infiltration rates out from BAS-grade CO_2 trend data without dosing a tracer gas (research question 3).

Table 3.5: Estimated average infiltration rates in the private office based on CO_2 concentration data measured from 2019 to 2020.

2019 - 2020	
Average Infiltration Rates (h^{-1})	R^2
0.7	0.9

It was found that the proposed method was not applicable for estimating infiltration rates by mixing historical humidity ratio data. The indoor environmental data (i.e., indoor RH and temperature) used to calculate the humidity ratio were measured by the BAS-grade sensor, whereas the outdoor environmental data (i.e., outdoor RH and temperature) were collected from Ottawa International Airport. Since the outdoor environmental data were greatly discrepant over time and the model's accuracy is dependent on the outdoor humidity ratio, three individual days were extracted from February 2021 to verify research question 3. These days were selected based on the criteria that the humidity ratio continuously declined after the AHU was completely shut down. In this case, the lowest indoor humidity ratio was set as the outdoor humidity ratio as the indoor humidity level approached the outdoor level because of infiltration.

Figure 3.10 illustrates the decay trend of the indoor humidity ratio and the linear correlation based on equation 6. The humidity ratio-based infiltration rates in Office 2 on three selected days are 0.38 h^{-1}, 0.28 h^{-1}, and 0.31 h^{-1}, respectively, which are less than the average CO_2-based estimate. Recall that the difference between CO_2-based and humidity ratio-based analysis is highly related to the adsorption and desorption mechanism of indoor material, which is discussed in detail in Section 3.4. R^2 values are all higher than 0.9, indicating that the proposed method appears to filter out infiltration rates from historical humidity ratio data on individual days (research question 3-3).

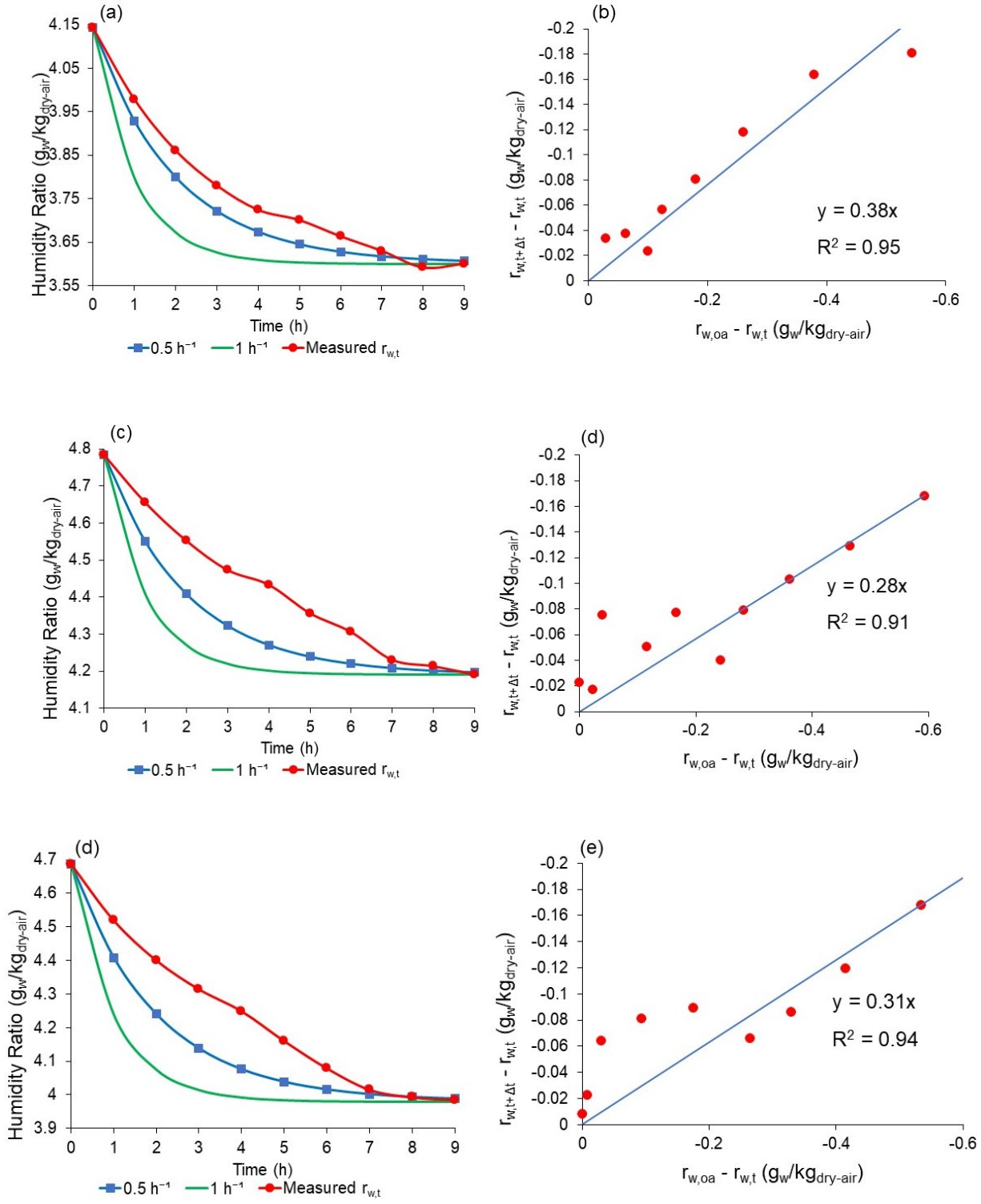

Figure 3.10:Indoor humidity ratio decay trend and infiltration rates estimated from (a) and (b) the first selected day, (c) and (d) the second selected day and (e) and (f) the third selected day.

Table 3.6 concludes humidity ratio-based infiltration estimates. Due to COVID-19, Office 2 was vacant for close to a year. This scenario reveals that the humidity ratio-based method is less dependent on occupant density than the CO_2-based method since the humidifier in the AHU keeps the indoor humidity constant when the AHU is in operation on cold days, even if the target area is vacant long-term.

Table 3.6: Infiltration estimates in the private office based on humidity ratio data taken from the BAS on three separate days.

	Average Infiltration Rates (h^{-1})	R^2
First selected day	0.38	0.95
Second selected day	0.28	0.91
Third selected day	0.31	0.94

Table 3.7 concludes all average infiltration rates calculated for Office 2 had different patterns. The deviations between average infiltration rates estimated from data measured using standalone data loggers and BAS sensors were less than 10% during tracer gas tests. For infiltration rates calculated by historical CO_2 data and CO_2 data measured by standalone data loggers, the maximum deviation was 15.6%, while the minimum deviation was 9%. The highest deviation between humidity ratio-based comparison (i.e., historical data and tracer gas testing data with standalone data logger) was 48%.

Table 3.7: Summary of infiltration estimates in the private office.

	Tracer Gas Test				Historical data	
	Data Logger CO_2 (h^{-1})	BAS Sensor CO_2 (h^{-1})	Data Logger r_w (h^{-1})	BAS Sensor r_w (h^{-1})	CO_2 (h^{-1})	r_w (h^{-1})
Day 1 (Tracer gas test)	0.83	0.78	0.54	0.51	-	-
Day 2 (Tracer gas test)	0.8	0.77	0.49	0.50	-	-
Selected five workdays	-	-	-	-	0.7	-
First selected day	-	-	-	-	-	0.38
Second selected day	-	-	-	-	-	0.28
Third selected day	-	-	-	-	-	0.31

3.3.4 Discussion

While our results demonstrate that inverse modelling with BAS-grade sensors (at least with CO_2 sensors) is a promising alternative to conventional tracer gas testing, certain factors may limit the generalizability of these findings to other buildings. The following paragraphs provide a discussion about these factors.

First, occupant density affects the accuracy of both historical CO_2 and humidity ratio analysis of the target zone. Occupant density is directly related to the continuous generation and accumulation of indoor CO_2 concentration and humidity level. Batterman [51] suggested several hundred ppm of CO_2 concentration rise (at least a 100 ppm change, but larger changes are beneficial) is necessary to narrow down the measurement errors. Therefore, a considerable indoor CO_2 increase is required for the inverse model-based approach to provide more reliable estimates. Since occupants exhale CO_2, which directly increases the indoor CO_2 concentration, the occupant density significantly influences indoor CO_2 measurements. In the present study, Office 2 was used by one occupant; thus, except for the occasional substantial increase due to academic activities (e.g., office hours and office meetings), the indoor CO_2 concentration usually had moderate growth. Same as CO_2 concentration, a larger increase of indoor humidity level produces more accurate infiltration estimates. The indoor humidity level rises during the operation of the humidifier in the AHU, and exhaled water vapour also helps increase the indoor humidity level. During the tracer gas test, the indoor RH level increased to 50% due to the intensive and continuous work of the humidifier, which was higher than the humidity on normal workdays (around 30%); thus, we captured a more notable decay trend than historical analysis. Note that the CO_2-based method is more dependent on occupant density than the humidity ratio-based method. As presented before, the infiltration estimates calculated by historical humidity ratio data suggest that the

humidity ratio-based method requires lower occupancy levels than the CO_2-based method if the humidifier in the AHU works periodically in winter.

Second, over-ventilation has more impact on the increase and accumulation of CO_2 concentration, in turn, on the accuracy of historical estimates. When the target zone is ventilated according to suggestions provided by ASHRAE 62.1 [63], the indoor CO_2 concentration should be at most 700 ppm higher than the outdoor level after the AHU is shut down. To be specific, this CO_2 difference (i.e., at most 700 ppm difference) decreases over time because of infiltration during unoccupied hours until the next morning working hours. If the target zone is over-ventilated, the accumulation of indoor CO_2 concentration will be reduced so that the CO_2 data collected by BAS-grade sensors will change insignificantly when the AHU is turned off. Since the academic building was over-ventilated, the historical CO_2 data obtained from Office 2 during unoccupied hours were less than 100 ppm difference. Therefore, only very rarely indoor CO_2 concentration was observed to be significantly greater than the outdoor CO_2 concentration, which leads to the difference between occupant-generated CO_2 results and tracer gas testing results.

Third, the humidity ratio-based analysis is more restricted by the adsorptive properties of the building interior. Moisture adsorption by indoor hygroscopic materials and furnishings directly influences the indoor humidity level. In the present study, a portion of indoor moisture may adhere to and accumulate on the surface of indoor hygroscopic materials such as walls, carpet, wood furniture, books, and so on; thus, the RH sensor can only measure the rest of the air moisture, which results in comparatively unreliable results. Desorption is another noticeable factor that can trigger the fluctuation of the indoor humidity level. As the molecules of water vapour are loosely held by the solid surface, they can easily leave the surface and return to the air. This is a potential explanation of the increase of humidity ratio during the decay phase in Figure 4 (b). Since the

adsorption and desorption rates are different for the various hygroscopic materials, the stability of indoor humidity level is difficult to control, which in turn causes the inaccuracy of humidity data. Giesbrecht et al. [13] suggested that the humidity ratio as tracer could be used in buildings that do not have too many moisture-adsorbing components and furnishings (e.g., extensive carpets and exposed unfurnished lumber) or might also be used in the constant injection and the constant concentration test instead of concentration decay method. It is worth noting that the proposed approach is intended merely as an operational tool providing a relative performance indicator of airtightness to benchmark and track infiltration characteristics over a building's life. By no means, is it intended as a substitute for conventional tracer gas tests. The humidity data gained from BASs can be helpful to track any changes in infiltration characteristics of a building over time if the CO_2 data are unavailable.

In summary, the considerable increase of occupant-generated CO_2 concentration and humidity ratio measurements are crucial when using the proposed approach in general conditions. The continuous generation and significant increase of CO_2 concentration and humidity ratio induce more reliable modelling results; however, they are considerably dependent on the occupant density, the ventilation, and the adsorption and desorption of indoor hygroscopic components of the target zone.

Occupants' behaviour is another factor that was not considered in the present study (fixed window) but may need to be considered when applying the proposed approach to buildings with operable windows. Different indoor environment comfort preferences allow occupants to behave variously, and occupants' behaviour randomly determines the state of windows. For instance, some occupants will choose to leave windows open to obtain additional ventilation requirements, while others may have opposite behaviours under the same condition. This situation leads to a decrease

in the indoor CO_2 concentration, which significantly influences indoor CO_2 measurements. More airflow can enter the building directly when windows are open, resulting in an overestimation of infiltration rates. However, high infiltration rates at this time cannot represent the poor airtightness of buildings. Occupants' behaviour was temporary, but the sensors, therefore, collected inaccurate data that affected modelling results.

As previously stated, several crucial prerequisites need to be highlighted because the applicability of the inverse model mentioned in the present study relies on the status of commercial buildings. First, to use the proposed approach, the AHUs should be turned off following a daily on-off schedule. To be clear, this method will not yield reliable results if the AHUs run 24 hours per day as the infiltration characteristics will be vastly different because of the building pressurization produced by mechanical ventilation systems and instead would measure a combination of infiltration and ventilation. It is also worth mentioning that a substantial amount of the air change rates measured during operational hours will result from ventilation which is a time-variant quantity based on the AHU operation modes. The typical ventilation rates in commercial buildings will be considerably higher than infiltration rates; hence it will become a mere noise in the BAS data when the building is pressurized. Distinguishing infiltration rates from total air change rates is a complicated process during this time. Meanwhile, the unknown number of occupants and their CO_2 and RH generation rates are also needed to determine the air change rate when the AHU is in operation. The proposed approach in this paper focuses on the non-operational hours to eliminate the effects of pressurization on the infiltration characteristics due to the mechanical ventilation system, to remove the impacts of ventilation considering its effectiveness and distribution into different zones, and to avoid the potential uncertainty regarding the occupant density. Otherwise, the inverse model will be more sophisticated as it requires data

for occupant counts and spatial distribution in each zone, CO_2 and RH measurements from AHU supply air, as well as the airflow rates at variable air volume terminals.

The second factor is that the target zone must be vacant after the AHUs are turned off. In this case, the target zone should be unoccupied to generate the decay of the indoor CO_2 concentration and humidity ratio, or the CO_2 and water vapour generated by occupants may lead to the indoor CO_2 and humidity ratio to continuously increase and affect the modelling results. Third, the indoor CO_2 concentration and the humidity ratio need to be tremendously above the outdoor levels so that the method can provide more reliable results. Fourth, this approach cannot yield reliable estimates in over-ventilated buildings. The indoor measurements are unable to reach the expected level due to over-ventilation. Also, the functionality of AHUs and sensors needs to be checked before employing the method, which directly impacts the collection of measurements. The inaccuracies due to sensor bias are allowed, but sensors should always be precise to ensure the consistent closeness of measurements to each other.

The novel approach introduced in this chapter measures the infiltration rates at a low cost and continuously detects the variation in building envelope with existing sensor-type data. It contributed to the aforementioned gaps in the literature regarding the use of simulation-based synthetic data and the lack of in-situ case studies by applying field-scale data to the inverse model-based approach. It should be emphasized that the proposed method is not developed to replace conventional tracer gas tests but as an operational tool for benchmarking and tracking the variation of infiltration characteristics. Therefore, this method can help building operators make the diagnosis on building maintenance and energy conservation, such as monitoring building airtightness in real-time and identifying potential problematic locations in the building. For instance, once the building airtightness degrades, the infiltration rates estimated through the

inverse model are expected to change as well. The variation in zonal infiltration estimates is also supposed to reflect the locations which have poor airtightness.

This research also confirmed standalone data loggers with recent calibration certificates could be replaced with BAS sensors, increasing the potential of using BAS-grade sensors built in thermostats and sensor hubs in tracer gas tests. This finding provides the flexibility of choice of measurement devices and allows experimental data to be more accessible through BASs. Furthermore, this paper also investigated the viability of using indoor humidity as a relative indicator of infiltration by using the inverse model-based method. According to the results estimated by tracer gas tests and the proposed method, the hygroscopic materials in the building interior are highly restrictive for the applicability of indoor humidity as a tracer gas due to the moisture adsorption and desorption dynamics. Nevertheless, the indoor humidity data can be treated as a complementary data source when the CO_2 data are unavailable to monitor the infiltration characteristics.

3.4 Closing remarks

Chapter 3 describes an inverse model-based approach developed to estimate the air infiltration rate in commercial buildings using CO_2 concentration and humidity ratio data. Compared with the conventional airtightness tests, this inverse modelling approach poses a cost-effective solution to continuously monitor infiltration rates by using ubiquitous sensor-type data. Furthermore, this method is easily adaptable to any commercial building if CO_2 or RH sensors are integrated within the BAS. The method was demonstrated through the tracer gas test data and historical data analysis involving a private office located in an academic building. The tracer gas test results indicate that the BAS-grade sensors are applicable for the proposed approach with

acceptable measurement errors. Besides, when specific prerequisites are satisfied, this approach appears to filter out the infiltration rates from existing sensor CO_2 and humidity ratio data. In accordance with the tracer gas test introduced in this study, the humidity ratio cannot be treated as a tracer gas due to moisture adsorption and desorption mechanism of hygroscopic materials, while it can help to track infiltration characteristics of a building over time when the CO_2 data are unavailable.

The inverse model is recommended for non-working hours on workdays, and several highlights may affect the application of the inverse model-based approach. In the process of model utilization: 1) the AHU should be shut down; 2) the target zone should be vacant; 3) the concentration of the tracer gas should be considerably greater than the outdoor level; 4) the target zone should not be over-ventilated, and 5) the sensors should operate without any trouble. Specifically for using humidity ratio as tracer gas: 1) the target zone should have limited moisture adsorptive and desorptive furnishings; and 2) humidifiers installed in AHUs can help increase the indoor RH levels for vacant target zone.

Chapter 4 - Estimation of infiltration in commercial buildings based on existing CO_2 sensors: An inverse Approach

This chapter has been published as:

Estimation of infiltration in commercial buildings based on existing CO_2 sensors: An inverse Approach

Z. Xiong; H. B. Gunay; C.A.Cruickshank; A. Wills, *ASHRAE Transactions . 2021, Vol. 127 Issue 1, p30-37. 8p.*

4.1 Introduction

Building infiltration rates are known to be one of the most influential parameters on building energy performance. Research shows that infiltration is responsible for 15 to 30% of annual space heating energy consumption in single-family homes and up to 45% in multi-unit residential buildings in Finland[32]. Air infiltration has been identified as the third most influential factor affecting energy consumption in commercial buildings in the United States [33]. In addition to that, this parameter has a strong relationship with indoor environmental conditions. High infiltration rates, especially in cold climates, can trigger thermal discomfort, affect indoor relative humidity, degrade indoor air quality, and increase energy demand [32]. Moreover, the occurrence of moisture condensation in the building envelope components will increase due to the moisture accumulation caused by air infiltration [43].

4.1.1 Background and previous work

In an effort to reduce air infiltration in buildings, a substantial research effort has been devoted in the past 30 years, where infiltration of residential buildings is highlighted. During this period, airtightness testing has become very common in residential buildings. The airtightness

characteristics of buildings are often determined through a standard fan pressurization test in accordance with ASTM E779 – 10 [11]. However, this method is generally less compatible with commercial buildings since it necessitates additional fans to ensure uniform pressurization in the entire building, which can turn into a labour-intensive and costly experimental setup[48][50]. There are some other difficulties (such as obstacles in pinpointing envelope imperfections) that make the fan pressurization test less suitable for the commercial sector than the residential sector.

Tracer gas testing is another recommended method to track air leakage rates in recent years. According to the ASTM E741-11 [9], tracer gas testing is more applicable to be used when considering the weather conditions and building operation. Tracer gas testing is beneficial to measure infiltration rates without involving artificial conditions. However, an ideal tracer gas is bounded by specific conditions [18], such as the safety of using tracer gas, the ease of measurement, the discrimination from air mixture and so on. Most of the currently used tracer gases have limitations. For example, the common tracer gas sulphur hexafluoride (SF_6) has a global warming potential (GWP) of 22800 over 100 years; thus, its use as a tracer gas is banned in the European Union. Compared with SF_6, CO_2 is a potential alternative that can be implemented in multi-zone commercial buildings. CO_2 is non-explosive and non-toxic at low concentrations and has a relatively low GWP of 1 over 100 years. Meanwhile, CO_2 sensor data have become easily accessible in recent years due to the widespread use of building management systems (BMS) – primarily intended for demand-controlled ventilation implementations.

In order to address the limitations of conventional airtightness tests, an inverse model-based method is proposed in this study. According to the ASHRAE Handbook: Fundamentals [53], the two common inverse model formalisms are black-box and grey-box approaches. Research in

the literature shows various techniques to develop inverse model-based approaches for the estimation of infiltration rates.

Ng and Wen [54] developed a grey-box building airflow network model to estimate airflow rates based on CO_2 sensor data. The results show that the least-squares performed well in the test as a parameter estimation technique and that the estimated airflow rates were in good agreement with the synthetic values. Hong and Lee [55] aimed to calibrate EnergyPlus models and estimate air infiltration rate and internal thermal mass using a novel inverse modelling approach. The inverse models were build based on the zone air balance equation and optimized the existing calibration workflow and thus helps improve the accuracy of energy simulation. New inverse modelling algorithms were also developed by Li, Hg and Sofos [57] to investigate people count and air infiltration rates. The result estimated from CO_2 concentration was found to agree with the ground truth of people counts and infiltration rates.

4.1.2 Objective and document structure

Considering economic and labour factors, conventional airtightness tests are mostly adequate for small-scale residential rather than large commercial buildings. Moreover, the difficulties of computing changeable infiltration rates in commercial buildings are the main reasons that the infiltration rates used in energy simulation software are often considered as constant values. To this end, the objective of this paper is to propose a low-cost inverse model-based approach to estimate the air infiltration rate by using existing CO_2 sensors. The average infiltration rate of an entire building can be computed continuously according to the return air CO_2 concentration of an air handling unit and thus can help detect the change of building envelope airtightness over time.

This paper first introduces the mathematical principles of linear regression models and multiple linear regression models and the background information of the case study. Then, the results and discussion sections exhibit tables and figures provided by regression models. These regression models are employed to estimate average infiltration rates and explain the variability of infiltration rates with wind speed and the temperature difference between indoors and outdoors.

4.2 Methodology

The methodology follows three parts: formulate mathematical models, preprocess data, and estimate the infiltration rates.

4.2.1 Linear regression model

In a recently vacated building, after the mechanical ventilation systems turn off, assuming a single well-mixed zone, the following simple differential equation defines the CO_2 decay behaviour:

$$\frac{dC}{dt} = (C_t - C_{oa})\frac{q_{inf}}{V} \quad (4.1)$$

where C_t is indoor CO_2 concentration at time t, q_{inf} is the air infiltration rate in m^3/s (cmf), and V is the volume of the zone in m^3 (ft^3). Referring to ASHRAE Standard 62.1 [63], the outdoor CO_2 concentration $C_{\mathrm{oa}}$is treated as a constant 400 ppm. The bias in each CO_2 sensor is also reflected in the C_{oa}value. For example, if the lowest return air CO_2 concentrations for a specific sensor were recorded to be 380 ppm over a long period, then the C_{oa} is set to be 380 ppm. For multiple sensors, the outdoor CO_2 concentration C_{oa} is unique for each sensor, reflecting each sensor's bias.

Subsequently, Eqn. 4.1 is discretized using a first-order forward difference approximation:

$$C_{t+60\,min} - C_t = (C_t - C_{oa}) \cdot Q_{inf} \quad (4.2)$$

$$\Delta C_t = (C_t - C_{oa}) \cdot Q_{inf} \quad (4.3)$$

where the difference between C_{t} and $C_{\mathrm{t+60\,min}}$ represents the variation of CO_2 concentration in one hour and Q_{inf} is the air infiltration rate in air change per hour (ACH), note that Q_{inf} is the average infiltration rate, and it is the unknown parameter of this simple regression problem.

4.2.2 Multiple linear regression model

The multiple linear regression model is developed to capture the impact of wind speed and stack effect on air infiltration rate, shown in Eqn. 4.4.

$$\frac{\Delta C_t}{(C_t - C_{oa})} = S_{wind,t} \cdot a_1 + \left|T_{out,t} - 20\right| \cdot a_2 + a_3 \quad (4.4)$$

where $S_{\mathrm{wind,t}}$ is the average wind speed over the hour in m/s (mph), and $T_{\mathrm{out,t}}$ is the hourly outdoor temperature reported at the beginning of each hour in degrees Celsius (℃). The comfortable indoor temperature recommended by ASHRAE Standard 55 [64] ranges approximately from 19℃ (66°F) to 27℃ (81°F). Thus, the indoor temperature used in this multiple linear regression model is assumed constant at 20℃ that is also the general setpoint of indoor temperature. The terms a_1, a_2, and a_3 are the unknown parameters of this regression problem that we estimate.

4.2.3 Case study

A case study is conducted to train the proposed inverse-based approach. The regression models were applied to three government office buildings located in Ottawa, Canada. All three buildings were built between the 1950s and 1970s. Data applied in this study were obtained based on the operating conditions of AHUs and the relevant return air CO_2 data. Note that only one AHU was selected from each building. Two filtering criteria were applied to select meaningful data before training the model in order to avoid the impact of mechanical ventilation systems (i.e., the unoccupied period of the buildings):

(1) AHU should be shut down.

(2) CO_2 data should be higher than 400 ppm.

A year's worth of hourly interval dataset of return air CO_2 concentration of the three office buildings was utilized to investigate system-level infiltration rates. The sensing data used in this paper were gained from building management systems of the buildings, while wind speed and outdoor air temperature implemented in the multiple linear regression model came from the meteorological data file measured at Ottawa International Airport. The programming environment R was used to orchestrate the data preprocessing, model development, and data visualization.

4.3 Results

This section consists of two parts; the first presents the overall patterns of CO_2 concentration in the case study buildings, and the second details the results of average infiltration rates at the system level.

4.3.1 Distributions of CO_2 concentration

A typical time-series curve was plot as an example to illustrate the variation of CO_2 concentration over time that affected by air infiltration. Figure 4.1 shows the fluctuation of indoor CO_2 concentration due to the occupied status of Building A for five weekdays. In the morning, the CO_2 concentration increases during the working hours and reaches the maximum value when the building is highly occupied and decreases gradually after working hours.

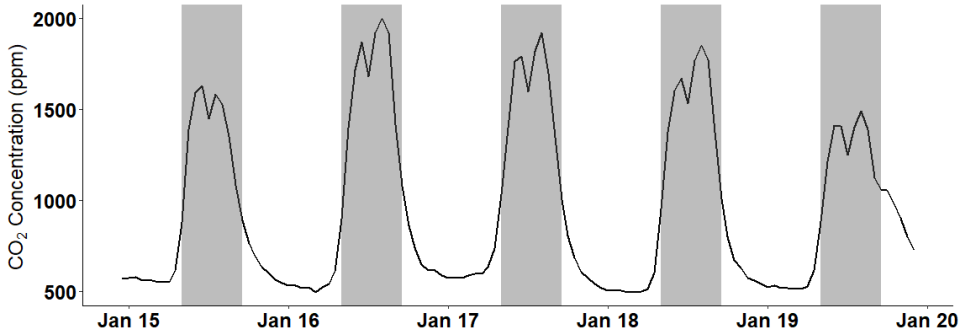

Figure 4.1: An illustrative example demonstrating the change in the CO_2 concentration of Building A over a week. The shaded regions indicate the working hours of each day from 8 a.m. to 5 p.m.

In order to observe the particular decay of CO_2 concentration with AHUs shut down (i.e., non-working hours), Figure 4.2 was built to illustrate the probability distributions of CO_2 concentrations in Building A, B, and C from 5 pm to 12 am in 2018 and 2019. Each curve represents the probabilities of CO_2 concentrations for a specific hour-of-the-day and tapers out at both tails with a peak that represents the mean value of CO_2 concentration calculated from the

yearly data. In summary, the distribution of CO_2 concentration in 2019 is narrower and sharper than that in 2018 for all buildings, which suggests that the air leakage of three buildings increases since they have a higher probability of reaching the mean CO_2 concentration and results in a higher infiltration rate that increases the speed of CO_2 decay. Besides, the decay in indoor CO_2 concentration during non-working hours is also influenced by the changes in the occupancy status of office buildings, considering the impact of occupancy on CO_2 concentration. On the other hand, the fluctuant outdoor CO_2 concentration and the varying wind speed and wind direction can also affect the variation of indoor CO_2 concentration.

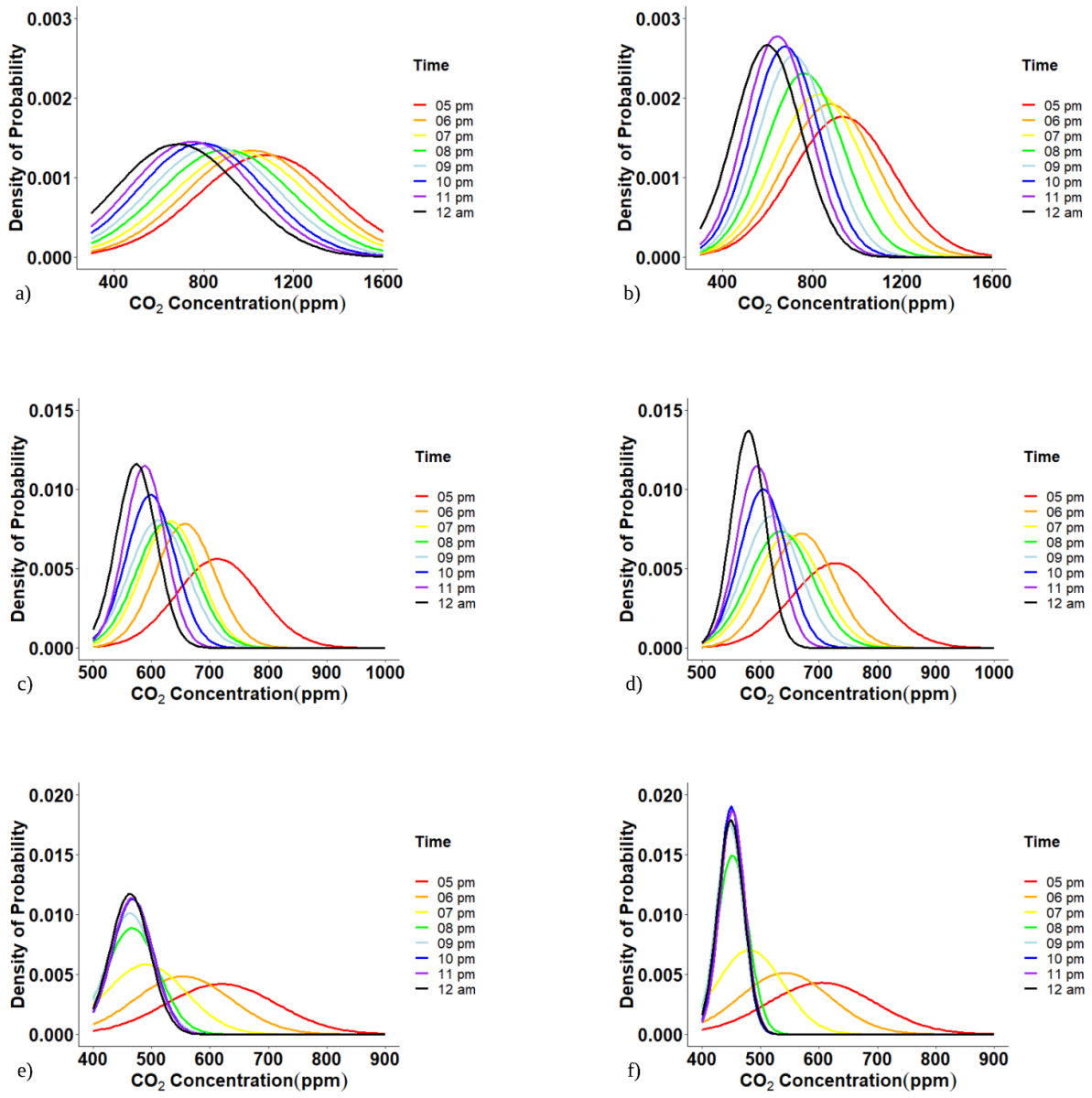

Figure 4.2: The probability of CO_2 concentration changing in the non-working time of workdays for Building A (a) in 2018 and (b) in 2019, for Building B (c) in 2018 and (d) in 2019, for Building C (e) in 2018 and (f) in 2019.

4.3.2 System-level air infiltration rates

4.3.2.1 Linear regression model

The linear correlation of two variables based on Eqn. 4.3 has been presented in Figures 4.3 (a) to 4.3 (f). The slope of each regression line represents the average air infiltration rate of each

building for two different years. One point in Figure 4.3 is especially worthy of notice. The Eqn. 4.3 was multiplied by an additional -1 to obtain positive average infiltration rates, which also resulted in negative values of the x-axis and y-axis. The summary of estimated average infiltration rates of three government office buildings and their statistical significance are shown below.

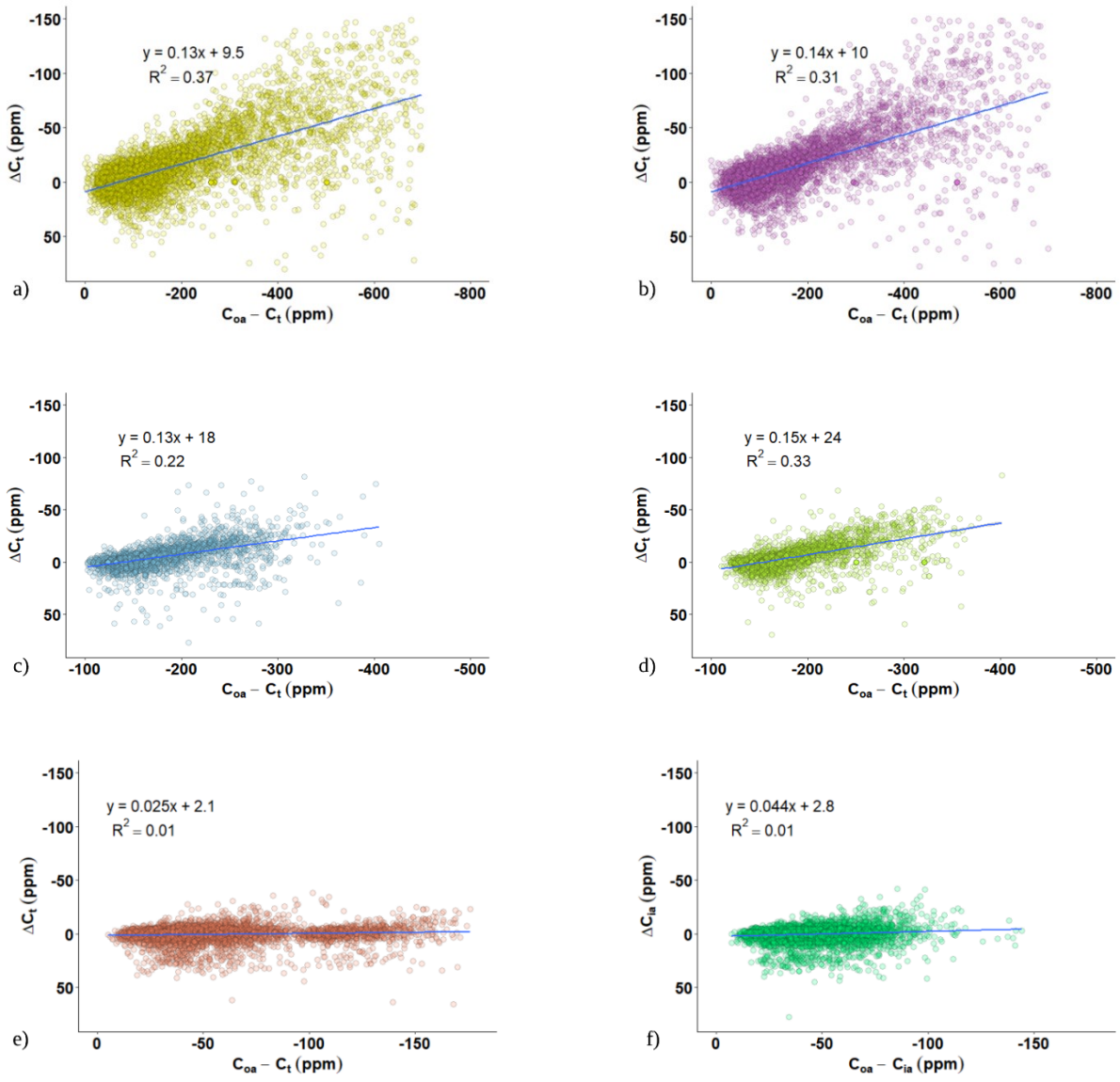

Figure 4.3: The average air infiltration rate represented by the slope of the trend line between hourly indoor CO_2 concentration difference and the CO_2 concentration difference between indoor and outdoor for Building A (a) in 2018 and (b) 2019, for Building B (c) in 2018 and (d) 2019, for Building C (e) in 2018 and (f) 2019.

Table 4.1 summarizes the estimated air infiltration rate, the p-value and the R^2 for each building. For Building A and Building B, the air infiltration rates in 2019 were slightly higher than those in 2018. The air infiltration rate of Building C in 2019 is nearly two times higher than that in 2018. The independent variable of this linear regression model is statistically significant since its p-values of all buildings are less than 0.05, which indicates that the variation in the independent variable ($C_{oa} - C_t$) correlates strongly with a shift in the dependent variable (ΔC_t). However, R^2 values are relatively low (ranged from 7% to 37%). Specifically, lots of factors can attribute to the significant variation that exists between measured infiltration rates and average infiltration rates, such as wind speed and stack effects. A multiple linear regression model was next applied to incorporate wind speed and the temperature difference between indoor and outdoor in the next subsection.

Table 4.1: R-squared and p-value for each building in 2018 and 219

Building	Average infiltration (ACH)		p-value		R^2	
	2018	2019	2018	2019	2018	2019
A	0.13	0.15	0.00	0.00	0.37	0.31
B	0.13	0.14	0.00	0.00	0.22	0.33
C	0.03	0.04	0.00	0.00	0.01	0.01

4.3.2.2 Multiple linear regression

Using Eqn. 4.4, the coefficients of each predictor of the multiple linear regression model are tabulated in Table 4.2. The wind speed coefficient (a_1) reflects the average effect on the air infiltration rate of one unit in wind speed. Similarly, a_2 represents the change in air infiltration rate due to a change of one unit in the temperature difference between indoors and outdoors. Table 4.2 presents that the change in temperature difference between indoor and outdoor and wind speed does not significantly affect the air infiltration rate in Building A. The average air infiltration rate of Building B is slightly influenced by wind speed, albeit not by the temperature differences.

However, both wind speed and temperature differences have a noticeable effect on Building C in 2018.

Table 4.2: Coefficients of the multiple linear regression model for each building.

Building	Wind Speed		Temperature Difference		Intercept	
	a_1	p-value	a_2	p-value	a_3	p-value
A - 2018	0.03	0.67	0.00	0.52	0.06	0.07
A - 2019	0.00	0.96	0.00	0.30	0.07	0.04
B - 2018	0.00	0.00	0.00	0.00	0.00	0.00
B - 2019	0.00	0.00	0.00	0.00	0.00	0.01
C - 2018	0.01	0.00	0.00	0.00	0.00	0.00
C - 2019	0.01	0.00	0.00	0.02	0.00	0.00

4.4 Discussion

The low R^2 values tabulated in Table 4.1 reflect that the linear regression model greatly limits the range of data selection that is unable to capture the nonlinear data. A single average infiltration rate may not be able to demonstrate system-level hourly variations of infiltration caused by wind speed, outdoor air temperature, and the status of unmeasured intentional envelope openings (e.g., windows left open).

A multiple linear regression model was implemented at the system level, considering the impact of wind speed and stack effects on infiltration rates. According to Table 4.2, high p-values and the coefficients of predictors approaching zero represent that the change in temperature difference and wind speed does not significantly affect the air infiltration rates. Theoretically, wind speed and infiltration are positively correlated (e.g., higher wind speed, higher infiltration rates), but time-varying wind direction, building orientation, surrounding landscape and buildings, and sensor positions may mask the impact of wind speed. Another possible reason is that the meteorological data applied in the multiple linear regression model was collected at Ottawa International Airport, which is far from the buildings of this study. Thus, the off-site weather data

may not reflect the real weather conditions of building sites.

4.5 Closing remarks

This study develops an inverse model-based approach to estimate average infiltration rates in commercial buildings using CO_2 concentration data. Compared with the conventional airtightness tests, this inverse modelling approach poses a cost-effective continuous monitoring solution using a ubiquitous sensor type AHU return air CO_2. Moreover, this method is easily adaptable to any commercial buildings provided that there are CO_2 sensors integrated within the BMS system. The method was demonstrated through a case study (i.e., the system-level analysis) involving three large government office buildings. The models estimate average infiltration rates ranging from 0.03 ach to 0.13 ach; however, with a relatively low R^2 value. This represents that the infiltration rates exhibit a large variability over time – which was partly explained due to wind and stack pressures, at least in one of the buildings.

It should be emphasized that the influence of mechanical ventilation systems and the operation status of CO_2 sensors should be avoided in the process of model application. Therefore, the inverse model is recommended for non-working hours (when AHUs are off) rather than working hours. At the same time, it is also necessary to verify whether the CO_2 sensors are functional.

Chapter 5 - Conclusions

5.1 Summary

This research project proposed an inverse model-based approach to estimate air infiltration in commercial buildings using occupant-generated CO_2 and humidity measured through low-cost, ubiquitous BAS sensors. The summary of the main findings of each chapter and the answers to research questions are outlined in this section.

5.1.1 An inquiry into the replicability of SF_6 with CO_2 in tracer gas testing

Chapter 2 presented the tracer gas concentration decay tests conducted in the IARL facility at the National Research Council of Canada by using SF_6 and CO_2 as tracer gases, and expensive high-accuracy gas monitors and low-cost BAS-grade sensors as measurement devices. Meanwhile, different building pressurization levels (10 Pa and 15 Pa) and arrangements of envelope leakage locations (same wall, across room and different height) were applied during the experimental program. The research questions introduced in chapter 2 were highlighted below to display the main findings of this chapter:

- *Can high-cost and high-environmental impact tracer gases such as SF_6 be replaced with CO_2 in tracer gas tests?* The CO_2 and SF_6 were dosed through an injection system, and the variation of tracer gas concentration was measured simultaneously through a photoacoustic gas monitoring system. The air change rates estimated from repeated experiments at five sampling locations were used to apply two independent sample t-tests. In accordance with the two independent sample t-tests results, the *t-value* was less than the critical value, which indicated that the SF_6-based air change rates are not statistically different from the CO_2-based air change rate in all experimental scenarios. This represented

that the mean value calculated by SF_6-based air change rates differed insignificantly from that calculated by CO_2-based air change rates in all experimental scenarios. It was concluded that CO_2 could be used as an alternative to SF_6 in tracer gas tests considering the environmental impact of SF_6.

- *Can BAS-grade CO_2 sensors be used instead of high-accuracy CO_2 data loggers to estimate infiltration rates?* The variation of CO_2 concentration was also measured by the photoacoustic gas monitoring system and BAS-grade sensors concurrently after stopping the injection. The two independent sample t-test was also employed to determine the relationship between measurements obtained by devices with different sensor qualities. The *t-values* computed from the two independent sample t-tests were smaller than the critical t value in all experimental scenarios, which reflected that the mean values of air change rates measured by photoacoustic gas monitors and BAS sensors are not significantly different from each other. The results suggested that the low-cost BAS-grade sensor is applicable to instead expensive high-accuracy data loggers during tracer gas tests.
- *Does the difference between CO_2 and SF_6-based tracer gas tests remain consistent at different pressurization levels?* The impacts of pressurization level on the use of CO_2 and SF_6 in tracer gas tests were examined by comparing the average difference of SF_6 and CO_2-based analysis at different building pressures. The differences of average air change rates were calculated at 10 Pa and 15 Pa, respectively, with the same arrangement of envelope leakage locations. The SF_6-based difference was quite similar to the CO_2-based difference at two test pressurization levels. Thus, the conclusion can be drawn based on the results of chapter 2 that the CO_2 is capable of being treated as tracer gas regardless of the pressurization levels of the test space.

- *Does the difference between CO_2 and SF_6-based tracer gas tests remain consistent when the air leakage locations are altered?* In order to discover the effect of envelope building leakage locations on using CO_2 and SF_6 as a tracer gas, the experiments were repeated with different combinations of motorized dampers that were used to simulate different building leaks. The difference of average air change rates was obtained from different air leakage locations at the same building pressure as was calculated. The results showed that the CO_2 and SF_6-based differences are acceptable when various leakage location arrangements are employed. It concluded that during tracer gas tests, the use of CO_2 and SF_6 is insensitive to envelope leakage locations.

5.1.2 An inquiry into the use of indoor CO_2 and humidity ratio trend data with inverse modelling to estimate air infiltration

To continuously monitor the air infiltration in commercial buildings, chapter 3 developed an inverse model-based approach to estimate infiltration rates through the occupant-generated CO_2 and humidity data when the building is unoccupied. As detailed in chapter 2 that CO_2 can be used as a tracer gas, while this chapter investigated the potentiality of using humidity as a tracer gas too. To this end, the CO_2 and humidity ratio-based tracer gas tests were carried out in an academic building to validate the proposed approach. The historical CO_2 and humidity data captured from the same building were applied to the proposed approach to filter out the infiltration rates. Using historical data allows us to assess the infiltration rates from naturally occurring CO_2 and humidity data without injecting a tracer gas. The research questions presented in chapter 3 were answered below:

- *Can the BAS-grade CO_2 sensors be used to estimate air infiltration rates instead of standalone CO_2 data loggers?* The CO_2 data were acquired from the two-day tracer gas

tests conducted in three private offices in an academic building after the mechanical ventilation system was shut down. A data logger was placed in each office to measure CO_2 data; in addition, there were built-in CO_2 and RH sensors in the BAS thermostat. The inter-sensor variations calculated from CO_2-based analysis were used as the indicators to compare tracer gas test results measured by different devices. The results exhibited that the inter-sensor variations were small (i.e., 0.05 h^{-1} on Day 1 and 0.03 h^{-1} on Day 2), which represented that the CO_2 concentration measured by two devices is generally consistent with an acceptable difference. Thus, the results suggested that the BAS-grade sensors were able to estimate infiltration rates in lieu of standalone data loggers.

- *Can humidity ratio (r_w) be treated as a tracer gas for estimating infiltration?* During the tracer gas testing carried out on Day 1 and Day 2, the fluctuation of indoor RH data was measured by BAS-grade sensors and standalone data loggers as well and was used to calculate humidity ratio (Eqn. 3.3 – 3.6). The p-values (i.e., zero for two days) and R^2 (i.e., 0.98 and 0.99 for standalone data loggers; 0.99 and 0.94 for BAS-grade sensors) demonstrated that the humidity ratio was a potential tracer gas in the tracer gas test. The highest difference between CO_2 and humidity ratio-based analysis was 0.29 h^{-1} on Day 1, indicating that although the humidity ratio was capable of being treated as a tracer gas, it was restricted by the absorptive properties of the building materials. Giesbrecht et al. [13] concluded that the moisture-absorbing components and furnishings were suggested to be avoided during tracer gas tests since they would affect the accuracy of tracer gas tests using humidity ratio.
- *Can an inverse model filter out the infiltration rates from BAS trend data for CO_2 and humidity ratio?* The historical data, including CO_2 and RH data, were extracted from the

same office (Office 2) and used to check whether the inverse model-based approach is applicable to filter out infiltration rates from occupant-generated CO_2 and humidity patterns without dosing a tracer gas. The historical CO_2 data were captured from five workdays in winter after the AHU was shut down. The CO_2-based average infiltration rates (0.7 h^{-1}) were estimated with an R^2 value of 0.9, which was close to the tracer gas test results using CO_2 (0.77 to 0.83 h^{-1}). This demonstrated that the method was able to filter out infiltration rates from historical CO_2 data. The historical humidity ratio data were obtained from three individual days. The results did not agree with CO_2-based results well, indicating that the proposed method cannot filter out infiltration rates from historical humidity ratio data.

5.1.3 Estimation of Infiltration in Commercial Buildings Based on Existing CO_2 Sensors: An Inverse Approach

Chapter 4 aimed to demonstrate the inverse model-based approach on a case study. A year's worth of CO_2 data was measured through CO_2 sensors installed in the return air duct of AHU, and three government office buildings in Ottawa were chosen as test buildings. The effect of wind speed and outdoor temperature on the inverse model-based infiltration estimation approach was investigated. The research questions solved in this chapter were detailed as follows:

- *Can the inverse model-based approach filter out system-level infiltration rates through naturally occurring CO_2 data?* The return air CO_2 measurements were gained from AHUs of government buildings, and for each building, only one AHU was selected to provide historical data. The following filtering criteria were applied to pick out desired CO_2 data: the AHU is shut down, and the indoor CO_2 concentration is higher than 400 ppm. The low R^2 values showed that the proposed model could only explain 7% to 37% variation of

mixing CO_2 data. Therefore, the single average infiltration rates were deemed to be incapable of explaining the variation caused by wind effect, stack effect as well as intentional openings.

- *Does weather condition affect the infiltration rates when the inverse model-based approach is implemented?* The wind speed and indoor-outdoor temperature data were applied to the multiple linear regression model (i.e., Eqn. 4.4) for the purpose of exploring the influence of stack and wind-driven pressures on the proposed method. Based on the coefficients and p-values of multiple linear regression model for each building, the wind speed and temperature difference between indoor and outdoor did not have a statistically significant effect on the average infiltration rates in Building A, since the p-values were greater than 0.05, and the wind speed and temperature difference coefficients approached to zero. The p-values of the other two buildings were smaller than 0.05, but the wind speed and temperature difference coefficients were still close to zero. Surprisingly, the results suggested that wind speed and temperature difference did not affect the whole-building infiltration estimates calculated from the inverse model-based approach. Note that several potential factors were not considered in this chapter, including wind direction, building orientation, site-specific weather data, and occupants' behaviour.

5.2 Research contributions

5.2.1 An inquiry into the replicability of SF_6 with CO_2 in tracer gas testing

The tracer gas tests conducted in the IARL contributed to the investigation of characteristics of CO_2 and SF_6 as tracer gas at different building environments. The laboratory tracer gas concentration tests examine the appropriateness of replacing SF_6 with CO_2 at different

pressurization levels and envelope leakage locations. This provides researchers more detailed criteria for selecting tracer gases between SF_6 and CO_2 so that they can decide the desired tracer gas more easily in terms of the building pressurization and envelope leakage locations. Furthermore, the analysis of impacts of sensor quality on CO_2-based tracer gas tests provides strong evidence for the use of low-cost CO_2 sensors integrated with BAS in tracer gas tests rather than using expensive high-accuracy measurement devices. This allows researchers to choose experimental instruments with more flexibility and comparatively reduces experimental budgets.

5.2.2 An inquiry into the use of indoor CO_2 and humidity ratio trend data with inverse modelling to estimate air infiltration

Chapter 3 focuses on the development of an inverse model-based approach used to estimate infiltration rates in commercial buildings. The proposed approach has three main contributions. First, the inverse model-based approach allows algorithms embedded in building energy management systems to automatically filter out infiltration rates using occupant-generated CO_2 and humidity data. It allows facility managers to monitor the infiltration rates through existing data infrastructure rather than relying on manual, invasive, and costly tracer gas experiments.

Second, this chapter confirms the effectiveness of humidity ratio as a potential tracer gas and highlights the noticeable points when applying it. It can be used as an alternative to monitoring the change in infiltration rates over time when CO_2 data are unavailable even though the efficacy is lower than using CO_2. Third, it demonstrates that the BAS-grade CO_2 and RH sensors can replace standalone data loggers in filed tracer gas tests and provides the potentiality of more use of CO_2 and RH sensors in thermostats and sensor hubs. These findings are under review for publication in *Building and Environment* as “An inquiry into the use of indoor CO_2 and humidity ratio trend data with inverse modelling to estimate air infiltration”.

5.2.3 Estimation of infiltration in commercial Buildings Based on Existing CO_2 Sensors: An Inverse Approach

Chapter 4 provides a case study of using the inverse model-based approach to estimate system-level infiltration rates in three government office buildings using existing CO_2 data. The method was used to calculate the average whole-building infiltration rates. The implementation of the proposed method confirms that this method can reflect the change in infiltration rates over time. The effect of outdoor temperature and wind speed was inspected through a multiple linear regression model, and they were deemed not to significantly affect the average whole-building infiltration rates. Future research should demonstrate the method through case studies featuring zone-level CO_2 and humidity sensors. These results were published as "Estimation of infiltration in commercial Buildings Based on Existing CO_2 Sensors: An Inverse Approach" in *ASHRAE Transactions*, and presented at ASHRAE's 2021 Winter Conference in Chicago, Illinois.

5.3 Recommendations for future work

In performing the research, the author identified a few potential points worth investigating in the future:

- The author recommends examining the effects of wind speed and outdoor temperature by using local weather station data. The investigation of wind and stack effect was based on the off-site meteorological data, which cannot reflect the time-varying weather conditions at the test location. The real-time weather data are more representative to examine the influence of wind and stack pressures on the proposed method.
- The inter-zonal air exchange between adjacent rooms needs to be investigated. In the present study, the air exchange was neglected between adjacent offices and the other

uncontrolled openings like the diffusers on the ceiling, the gap under the door, and cracks of building structures. The fluctuation of historical occupant-generated CO_2 and humidity data caused by inter-zonal airflow cannot be indistinguishable, which is possible to reduce the sensitivity of the model to infiltration caused by envelope leaks. To this end, advanced modelling may be needed in future studies to evaluate the inter-zonal air exchange rates through unintentional openings.

- The occupants' behaviour is also a noticeable factor that needs to be considered in future works. The study presented in chapter 3 was based on the data collected from the building with fixed windows. However, for buildings with operable windows, for example, the government office buildings mentioned in chapter 4, results rely highly on window states. Once occupants leave windows open, the air flows into the building will affect air change rates, in turn, reduce the reliability of the inverse model-based approach.
- The inverse model-based approach should be tested with different environmental scenarios using airflow network modelling. The data used in this research, including experimental data and historical data, were collected in Ottawa. Moreover, the experimental data are from different seasons. Therefore, the synthetic data generated for a wide range of environmental conditions using airflow network modelling enables this method's worldwide application in different climates.

Reference

[1] US Department of Energy, "Windows and Building Envelope Research and Development: Roadmap for Emerging Technologies," 2014.

[2] S. J. Emmerich and A. K. Persily, "Analysis of U.S. commercial building envelope air leakage database to support sustainable building design," *Int. J. Vent.*, vol. 12, no. 4, pp. 331–343, 2014.

[3] C. H. Lozinsky and M. F. Touchie, "Inter-zonal airflow in multi-unit residential buildings: A review of the magnitude and interaction of driving forces, measurement techniques and magnitudes, and its impact on building performance," *Indoor Air*, vol. 30, no. 6, pp. 1083–1108, 2020.

[4] A. K. Persily, "Field measurement of ventilation rates," *Indoor Air*, vol. 26, no. 1, pp. 97–111, 2016.

[5] C. H. E. Harderup, "Moisture Conditions in a North Facing Wall with Cellulose Loose Fill Insulation: Constructions with and without Vapor Retarder and Air Leakage," *ASHRAE Trans.*, vol. 101, pp. 228–243, 1995.

[6] A. Janssens and H. Hens, "Interstitial Condensation Due to Air Leakage: A Sensitivity Analysis," *J. Build. Phys.*, vol. 27, no. 1, pp. 15–29, 2003.

[7] NECB 2017, *National Energy Code of Canada for Buildings*, National Research Council of Canada, Ottawa, ON, Canada, 2017.

[8] H. B. Gunay, "Infiltration," presented to the class, Carleton University, Ottawa, ON, Canada, 2020. [*PowerPoint slides*]. Accessed on: Aug. 9. 2021.

[9] ASTM E741-11, *Standard Test Method for Determining Air Change in a Single Zone by Means of a Tracer Gas Dilution*, ASTM International, West Conshohocken, PA, USA, 2017.

[10] S. Thébault and J. R. Millet, “Cost-effective air flow rate estimations using blowerdoor and wind speed measurements to assess building envelope thermal performances,” *J. Build. Phys.*, vol. 40, no. 6, pp. 504–529, 2017.

[11] ASTM E779-19, *Standard Test Method for Determining Air Leakage Rate by Fan Pressurization*, ASTM International, West Conshohocken, PA, USA, 2019.

[12] M. H. Sherman, “Tracer-gas techniques for measuring ventilation in a single zone,” *Build. Environ.*, vol. 25, no. 4, pp. 365–374, 1990.

[13] J. C. Giesbrecht, F. A. Curtis, and T. Viraraghavan, “Water vapour as a tracer for ventilation rate measurements,” *Int. J. Environ. Stud.*, vol. 56, no. 2, pp. 171–185, 1999.

[14] M. G. Marley, “The measurement of the rate of air change,” *J. Inst. Heat. Vent. Eng.*, 1935.

[15] B. G. Collins and D. B. Smith, “The Measurement of Ventilation Rates using a radioactive Tracer,” *J. Inst. Heat. Vent. Eng.*, vol. 23, pp. 270–274, 1955.

[16] A. H. Howland, D. E. Kimber, and R. F. Littlejohn, “Measurements of Air Movements in a House using a radioactive Tracer Gas,” *J. Inst. Heat. Vent. Eng.*, pp. 57–70, 1960.

[17] M. Samer, H. J. Müller, M. Fiedler, W. Berg, and R. Brunsch, “Measurement of ventilation rate in livestock buildings with radioactive tracer gas technique: Theory and methodology,” *Indoor Built Environ.*, vol. 23, no. 5, pp. 692–708, 2014.

[18] S. Cui, M. Cohen, P. Stabat, and D. Marchio, “CO2 tracer gas concentration decay method for measuring air change rate,” *Build. Environ.*, vol. 84, pp. 162–169, 2015.

[19] D. T. Grimsrud, “An intercomparison of tracer gases used for air infiltration measurements,” *ASHRAE Trans.*, vol. 86, pp. 258–267, 1980.

[20] M. Hori and T. Mizoguchi, “Measurement of’ ventilation rate using tracer-Gas-decay

method with isobutene and photo ionization detector," *J. Environ. Eng.*, vol. 73, no. 626, pp. 451–455, 2008.

[21] H. Yoshino *et al.*, "Measurement of ventilation airflow rates of 39 houses by three different methods," *Int. J. Vent.*, vol. 8, no. 4, pp. 299–311, 2010.

[22] P. Keig, T. Hyde, and G. McGill, "A comparison of the estimated natural ventilation rates of four solid wall houses with the measured ventilation rates and the implications for low-energy retrofits," *Indoor Built Environ.*, vol. 25, no. 1, pp. 169–179, 2016.

[23] J. Dias Carrilho, M. Mateus, S. Batterman, and M. Gameiro Da Silva, "Air exchange rates from atmospheric CO2 daily cycle," *Energy Build.*, vol. 92, pp. 188–194, 2015.

[24] H. K. W. Mai, D. W. T. Chan, and J. Burnett, "Dynamic evaluation of airflow rates for a variable air volume system serving an open-plan office," *Indoor Air*, vol. 13, no. 3, pp. 311–312, 2003.

[25] C. Men, S. Wang, and Z. Zou, "Experimental study on tracer gas method for building infiltration rate measurement," *Build. Serv. Eng. Res. Technol.*, vol. 41, no. 6, pp. 745–757, 2020.

[26] U. Haverinen-Shaughnessy, D. J. Moschandreas, and R. J. Shaughnessy, "Association between substandard classroom ventilation rates and students' academic achievement," *Indoor Air*, vol. 21, no. 2, pp. 121–131, 2011.

[27] N. Muscatiello, A. Mccarthy, C. Kielb, W. H. Hsu, S. A. Hwang, and S. Lin, "Classroom conditions and CO2 concentrations and teacher health symptom reporting in 10 New York State Schools," *Indoor Air*, vol. 25, no. 2, pp. 157–167, 2015.

[28] C. T. Dervos and P. Vassiliou, "Sulfur hexafluoride (sf6): Global environmental effects and toxic byproduct formation," *J. Air Waste Manag. Assoc.*, vol. 50, no. 1, pp. 137–141,

2000.

[29] ASHRAE 62.2, *Ventilation and Acceptable Indoor Air Quality in Residential Buildings*, American Society of Heating, Refrigerating and Air-Conditioning Engineers, Atlanta, GA, USA, 2019.

[30] T. A. Reddy, *Applied Data Analysis and Modeling for Energy Engineers asn Scientists*. SpringerScience+Business Media, 2011.

[31] J. Berquist, A. Wills, I. MacDonald, C. Banister, M. Bartko, and M. Vuotari, "The effects of leakage location on building air change rate in a pressurized building," *ASHRAE Trans.*, vol. 126, pp. 409–418, 2020.

[32] J. Jokisalo, J. Kurnitski, M. Korpi, T. Kalamees, and J. Vinha, "Building leakage, infiltration, and energy performance analyses for Finnish detached houses," *Build. Environ.*, vol. 44, no. 2, pp. 377–387, 2009.

[33] M. Bhandari, D. Hun, S. Shrestha, S. Pallin, and M. Lapsa, "A simplified methodology to estimate energy savings in commercial buildings from improvements in airtightness," *Energies*, vol. 11, no. 12, pp. 1–16, 2018.

[34] T. Kalamees, "Air tightness and air leakages of new lightweight single-family detached houses in Estonia," *Build. Environ.*, vol. 42, no. 6, pp. 2369–2377, 2007.

[35] C. J. Ghazi and J. S. Marshall, "A CO2 tracer-gas method for local air leakage detection and characterization," *Flow Meas. Instrum.*, vol. 38, pp. 72–81, 2014.

[36] Y. Shi, X. Li, and H. Li, "A new method to assess infiltration rates in large shopping centers," *Build. Environ.*, vol. 119, pp. 140–152, 2017.

[37] W. Liu, X. Zhao, and Q. Chen, "A novel method for measuring air infiltration rate in buildings," *Energy Build.*, vol. 168, pp. 309–318, 2018.

[38] X. Zheng, E. Cooper, M. Gillott, and C. Wood, "A practical review of alternatives to the

steady pressurisation method for determining building airtightness," *Renew. Sustain. Energy Rev.*, vol. 132, no. July, p. 110049, 2020.

[39] A. M. Pessi, J. Suonketo, M. Pentti, M. Kurkilahti, K. Peltola, and A. Rantio-Lehtimäki, "Microbial growth inside insulated external walls as an indoor air biocontamination source," *Appl. Environ. Microbiol.*, vol. 68, no. 2, pp. 963–967, 2002.

[40] M. Airaksinen, P. Pasanen, J. Kurnitski, and O. Seppänen, "Microbial contamination of indoor air due to leakages from crawl space: A field study," *Indoor Air*, vol. 14, no. 1, pp. 55–64, 2004.

[41] S. J. Emmerich, J. E. Gorfain, and C. Howard-Reed, "Air and Pollutant Transport from Attached Garages to Residential Living Spaces – Literature Review and Field Tests," *Int. J. Vent.*, vol. 2, no. 3, pp. 265–276, 2003.

[42] S. M. Nazaroff, W.W.; Doyle, "Radon Entry Into House Having a Crawl Space," *Health Phys.*, vol. 48, no. 3, pp. 265–281, 1985.

[43] C. Younes, C. A. Shdid, and G. Bitsuamlak, "Air infiltration through building envelopes: A review," *J. Build. Phys.*, vol. 35, no. 3, pp. 267–302, 2012.

[44] S. Chen, M. D. Levine, H. Li, P. Yowargana, and L. Xie, "Measured air tightness performance of residential buildings in North China and its influence on district space heating energy use," *Energy Build.*, vol. 51, pp. 157–164, 2012.

[45] W. Pan, "Relationships between air-tightness and its influencing factors of post-2006 new-build dwellings in the UK," *Build. Environ.*, vol. 45, no. 11, pp. 2387–2399, 2010.

[46] V. Iordache, I. Nastase, A. Damian, and I. Colda, "Average permeability measurements for an individual dwelling in Romania," *Build. Environ.*, vol. 46, no. 5, pp. 1115–1124, 2011.

[47] CGSB-149.10-M86, *Determination of the airtightness of building envelopes by the fan depressurization method*, Canadian General Standards Board, Ottawa, ON, Canada, 2019.

[48] L. C. Ng, A. Musser, A. K. Persily, and S. J. Emmerich, "Multizone airflow models for calculating infiltration rates in commercial reference buildings," *Energy Build.*, vol. 58, pp. 11–18, 2013.

[49] G. Remion, B. Moujalled, and M. El, "Review of tracer gas-based methods for the characterization of natural ventilation performance : Comparative analysis of their accuracy," *Build. Environ.*, vol. 160, no. June, p. 106180, 2019.

[50] I. Turiel and J. Rudy, "Occupant-generated CO2 as an Indicator of Ventilation Rate," *Lawrance Berkeley Natl. Lab.*, 1980.

[51] S. Batterman, "Review and extension of CO2-based methods to determine ventilation rates with application to school classrooms," *Int. J. Environ. Res. Public Health*, vol. 14, no. 2, pp. 1–22, 2017.

[52] R. Claude-Alain and F. Foradini, "Simple and Cheap Air Change Rate Measurement Using CO 2 Concentration Decays," *Int. J. Vent.*, vol. 1, no. 1, pp. 39–44, 2002.

[53] ASHRAE, *ASHRAE Handbook - Fundamentals*, American Society of Heating, Refrigerating and Air-Conditioning Engineers, Atlanta, GA, USA, 2017.

[54] L. C. Ng and J. Wen, "Estimating building airflow using CO2 measurements from a distributed sensor network," *HVAC R Res.*, vol. 17, no. 3, pp. 344–365, 2011.

[55] T. Hong and S. H. Lee, "Integrating physics-based models with sensor data: An inverse modeling approach," *Build. Environ.*, vol. 154, no. January, pp. 23–31, 2019.

[56] M. Deru *et al.*, "U.S. Department of Energy commercial reference building models of the national building stock," *Publ.*, no. February 2011, pp. 1–118, 2011.

[57] H. Li, T. Hong, and M. Sofos, "An inverse approach to solving zone air infiltration rate and people count using indoor environmental sensor data," *Energy Build.*, vol. 198, pp. 228–242, 2019.

[58] Z. Xiong, B. Gunay, C. Cruickshank, and A. Wills, "Estimation of Infiltration in Commercial Buildings Based on Existing CO 2 Sensors : An Inverse Approach," *ASHRAE Winter Conf.*, 2021.

[59] H. Burak Gunay, D. Darwazeh, S. Shillinglaw, and I. Wilton, "Remote characterization of envelope performance through inverse modelling with building automation system data," *Energy Build.*, vol. 240, p. 110893, 2021.

[60] Onset Computer Corporation, Technical Data Sheet, HOBO MX1102A Data Logger for CO_2, Temperature, and Humidity Ratio.

[61] Delta, Technical Data Sheet, DNS-24 Room Sensor for Temperature, Humidity, Motion, and CO_2.

[62] S. Van Buggenhout, A. Van Brecht, S. Eren Özcan, E. Vranken, W. Van Malcot, and D. Berckmans, "Influence of sampling positions on accuracy of tracer gas measurements in ventilated spaces," *Biosyst. Eng.*, vol. 104, no. 2, pp. 216–223, 2009.

[63] ASHRAE 62.1, *Ventilation for Acceptable Indoor Air Quality*, American Society of Heating, Refrigerating and Air-Conditioning Engineers, Atlanta, GA, USA, 2013.

[64] ASHRAE 55, *Thermal Environmental Conditions for Human Occupancy*, American Society of Heating, Refrigerating and Air-Conditioning Engineers, Atlanta, GA, USA, 2017.